ＰＦ研究会「X線トポグラフィーの現状と展望」
ＫＥＫ４号館２階輪講室１，２
2011年1月11日（火）15:10 ~ 15:50

TEMによる転位の３次元分布観察

九州大学 大学院総合理工学研究院
波多　聰

Acknowledgements

光原昌寿、田中將己、池田賢一、金子賢治、中島英治、東田賢二、松村晶

友清芳二、桑野範之、板倉賢（九州大学）

宮崎裕也（メルビル）

宮崎伸介（日本FEI）

J. S. Barnard, J. H. Sharp, P. A. Midgley (University of Cambridge)

A. Ramar, T. Kasama, R.E. D.-Borkowski, X. Huang, G. Winther, N. Hansen

(CEN, RISØ, DTU, Denmark)

Financial Supports

Kyushu University, JSPS and MEXT, Japan

Outline

1. 回折コントラストによるTEMトモグラフィー観察法の検討

- ・回折条件設定と試料傾斜の両立 → ３軸トモグラフィーホルダー
- ・３次元観察に適した像コントラスト → 走査透過電子顕微鏡法STEM

2. 転位観察への適用

- ・オーステナイト鋼
- ・シリコン単結晶のクラック先端転位
- ・純アルミニウム多結晶の変形組織

Procedure of TEM/STEM tomography

Tilt series (TEM/STEM)

Specimen tilt: ±60° ~ ±80° (a special specimen holder necessary)
Increment: 1° ~ 4°
Total No. of images: 31 ~ 161
Projection requirement
(mass, thickness, etc.)

3D reconstruction (PC)

Align image shift in the tilt series
Determine the tilt axis
Reconstruct 3D volume using filtered back projection, SIRT, etc.

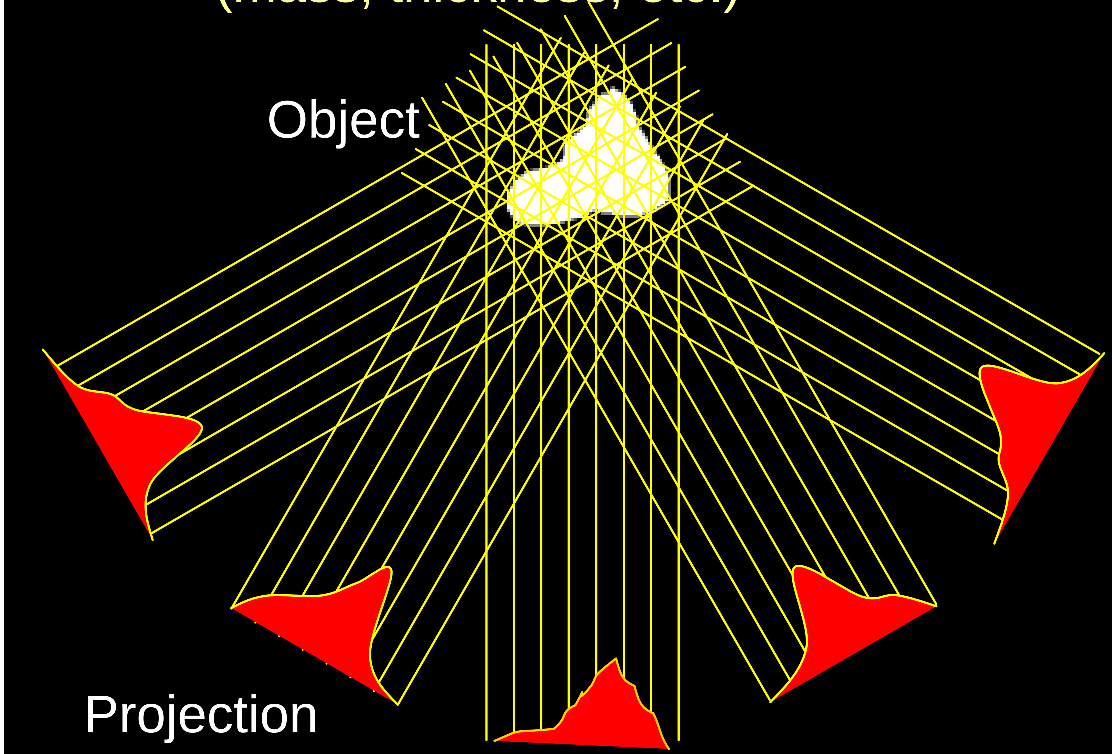

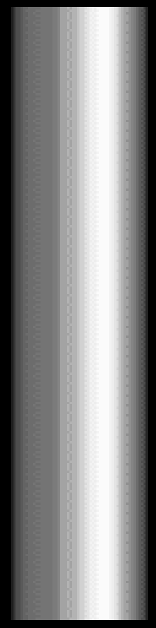

Back projection

Development of TEM tomography

Ziese and de Jong: Applied Catalysis A (2004)

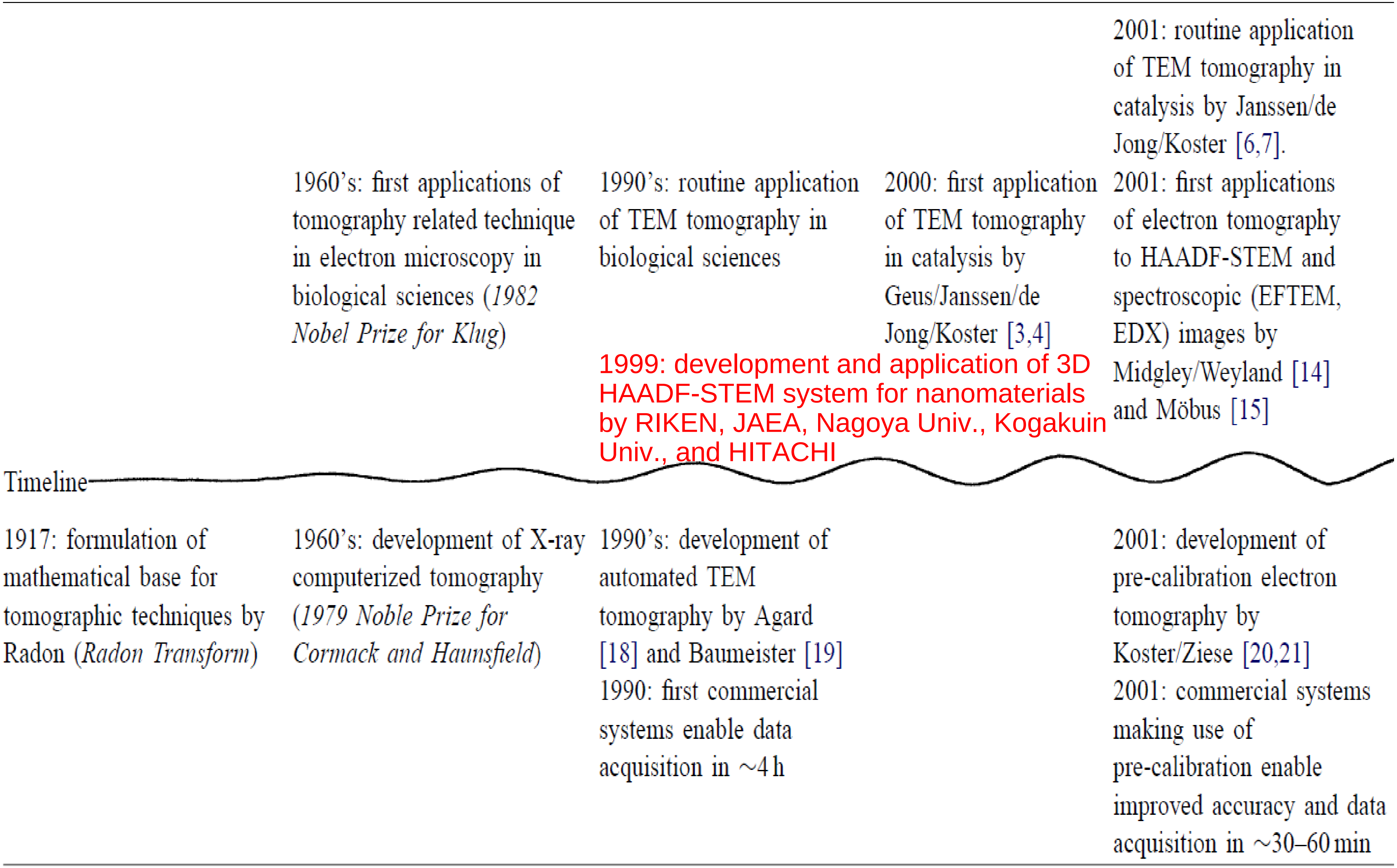

1960’s: first applications of tomography related technique in electron microscopy in biological sciences (*1982 Nobel Prize for Klug*)

1990’s: routine application of TEM tomography in biological sciences

2000: first application of TEM tomography in catalysis by Geus/Janssen/de Jong/Koster [3,4]

2001: routine application of TEM tomography in catalysis by Janssen/de Jong/Koster [6,7].

2001: first applications of electron tomography to HAADF-STEM and spectroscopic (EFTEM, EDX) images by Midgley/Weyland [14] and Möbus [15]

1999: development and application of 3D HAADF-STEM system for nanomaterials by RIKEN, JAEA, Nagoya Univ., Kogakuin Univ., and HITACHI

Timeline

1917: formulation of mathematical base for tomographic techniques by Radon (*Radon Transform*)

1960’s: development of X-ray computerized tomography (*1979 Noble Prize for Cormack and Haunsfield*)

1990’s: development of automated TEM tomography by Agard [18] and Baumeister [19]

1990: first commercial systems enable data acquisition in ~4 h

2001: development of pre-calibration electron tomography by Koster/Ziese [20,21]

2001: commercial systems making use of pre-calibration enable improved accuracy and data acquisition in ~30–60 min

Electron tomography for cell biology

Non-crystalline
Non-periodic
Complex
nanostructures

分解能
1 nm：単粒子解析
2~4 nm: TEM-CT
(Baumeister, IMC17 (2010)

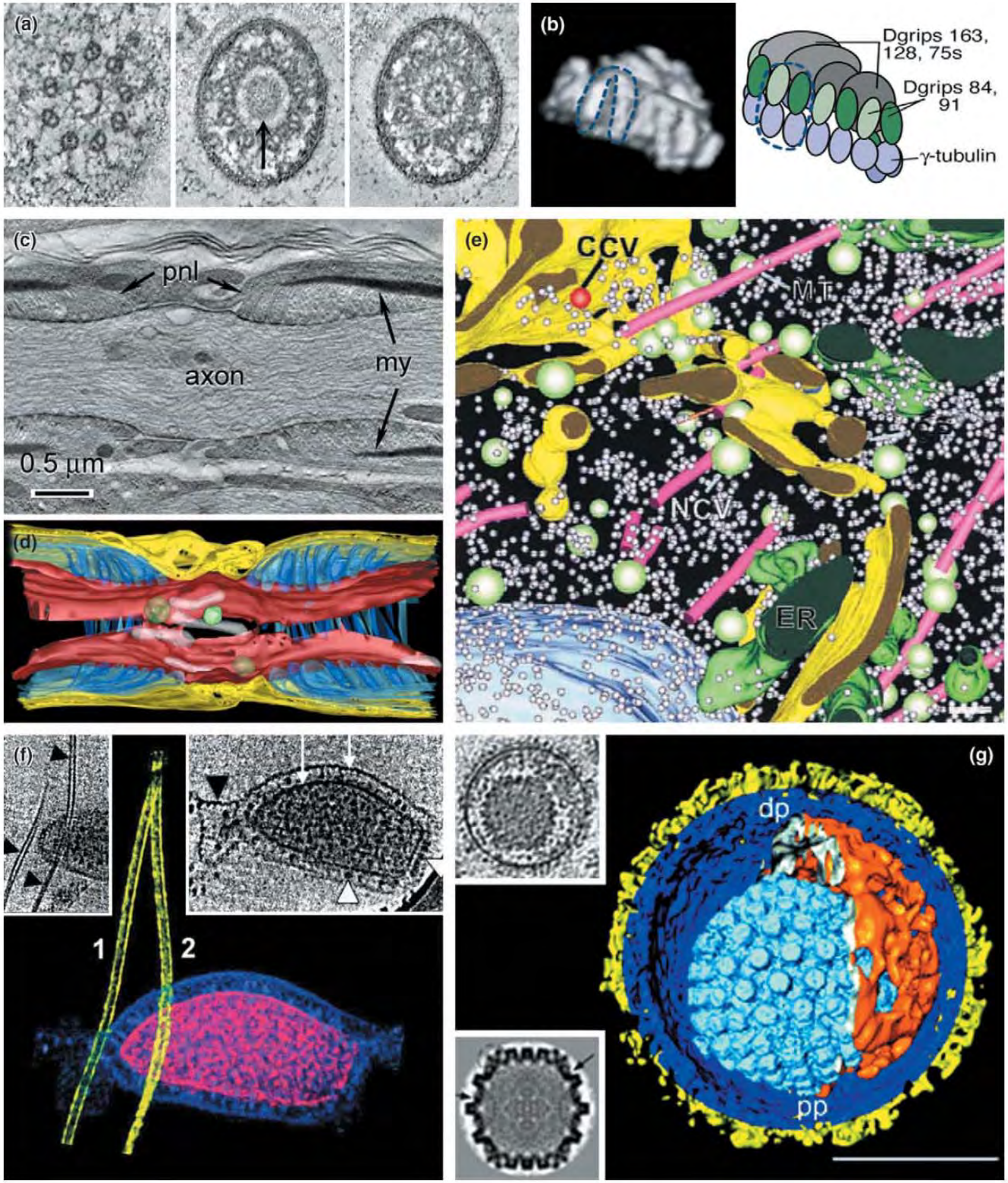

McIntosh et al.: TRENDS in Cell Biology (2005)

Electron tomography for nanoparticles

3D shape, volume connectivity and location of nano-pores inside a support material

1~2 nm resolution becomes in routine

Preliminary result of atomic-resolution TEM-CT
(IMC17, 09/2010)

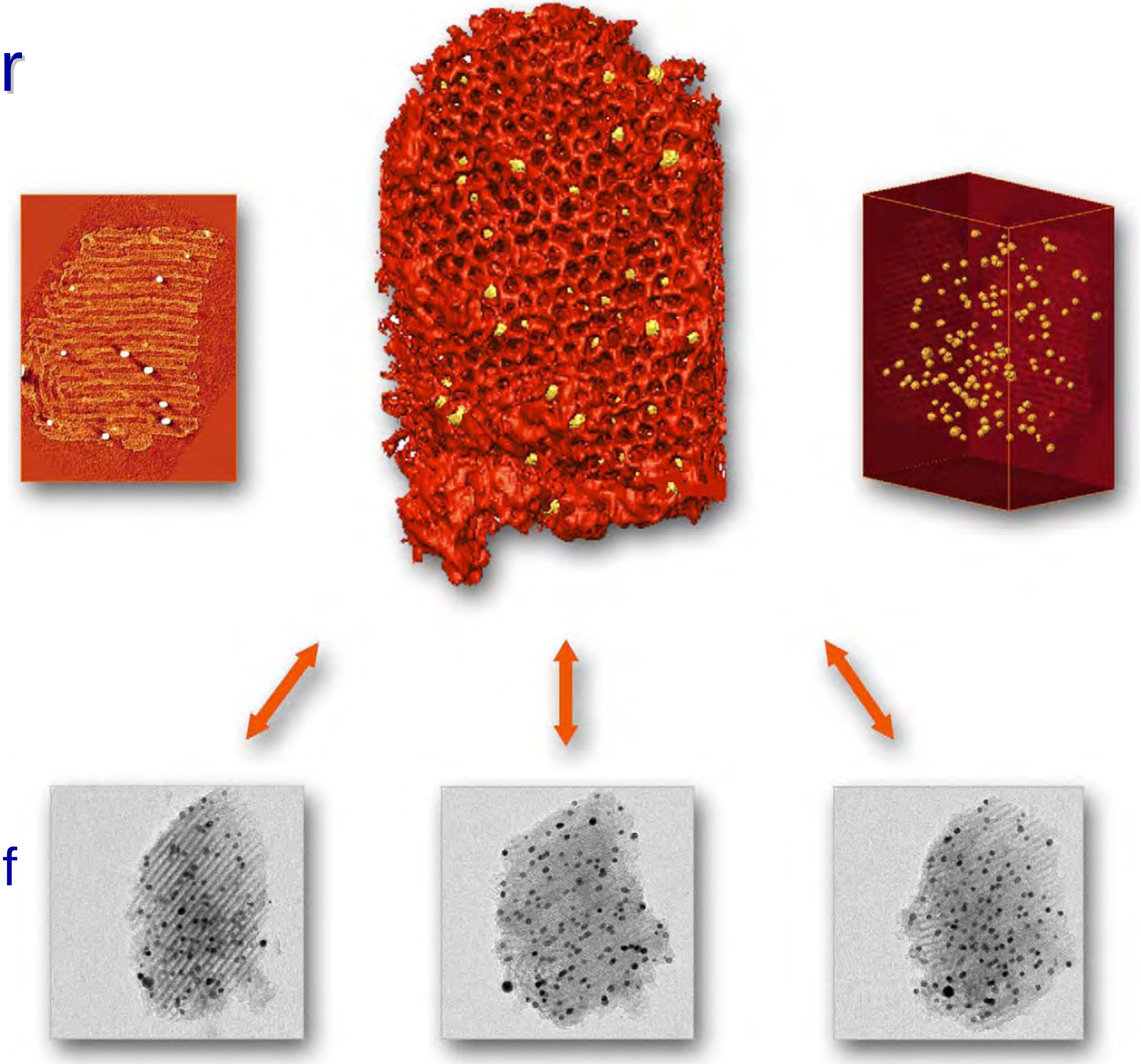

Ziese and de Jong: Applied Catalysis A (2004)

4D Electron Tomography

Oh-Hoon Kwon and Ahmed H. Zewail*

Fig. 4. 4D tomographic visualization of motion. (**A**) Representative 3D volume snapshots of the nanotubes at relatively early times. Each 3D rendered structure at different time delay (beige) is shown at two view angles. A reference volume model taken at *t* = 0 ns (black) is merged in each panel to highlight the resolved nanometer displacements. Arrows in each panel indicate the direction of motion. (**B**) The time-dependent structures visualized at later times and with various colors to indicate different temporal evolution. The wiggling motion of the whole bracelet is highlighted with arrows. From these tomograms, movies were constructed in the two different time domains (movies S2 and S3). Note that the time scale given here is chosen to display clearly the objects' motions, as opposed to the early ultrashort time domain (see text).

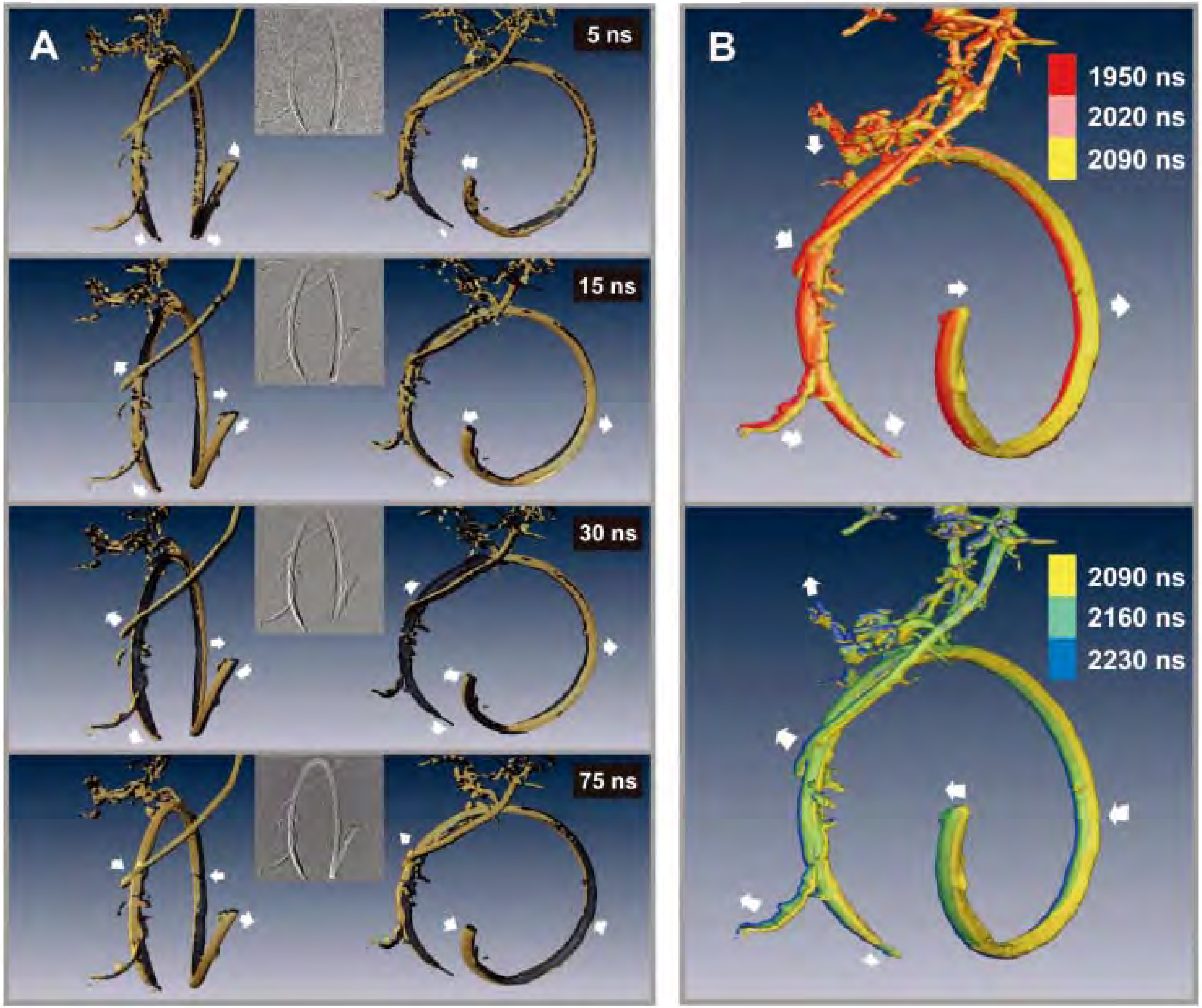

CNTの弾性変形

パルス照射（熱、電子）、超高速撮像とTEMトモグラフィーの融合

TEM tomography using diffraction contrast

Visualize microstructure in crystals (Mass-thickness contrast is not appropriate)

Dark-field TEM tomography for ordered structures

Imaging of superlattice domain structure

Kimura *et al.*: *J. Electron Microsc.* (2005)

Hata *et al.*: *Adv. Mater.* (2008)

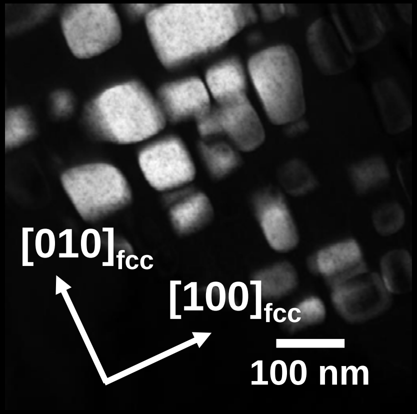

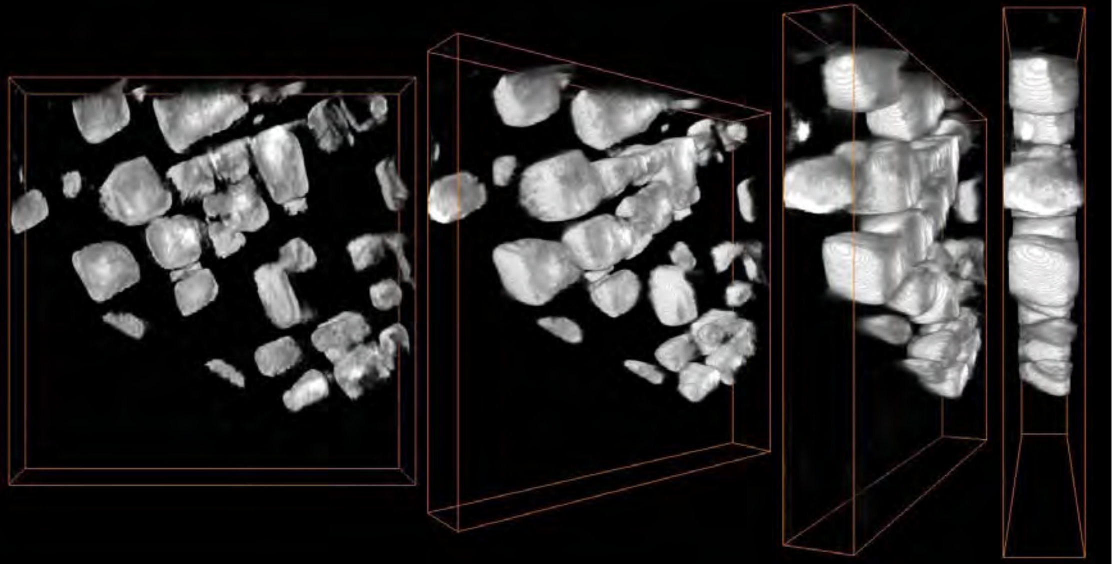

Weak-beam dark-field TEM tomography for dislocations

Dislocation networks in GaN film

Barnard *et al*: *Science* & *Philos. Mag.* (2006)

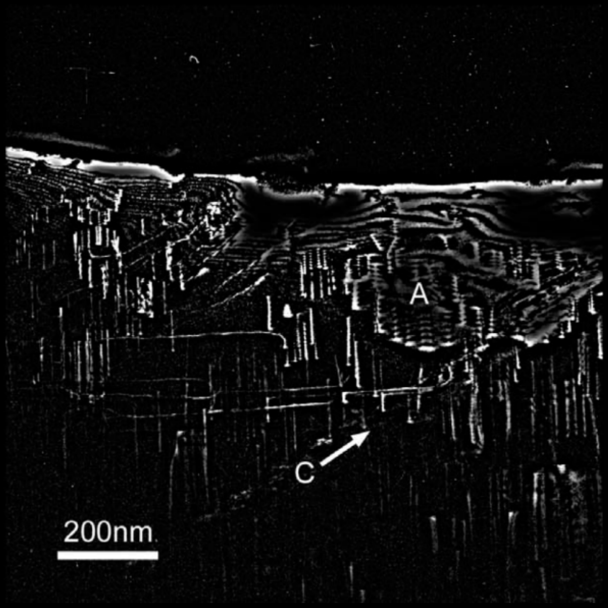

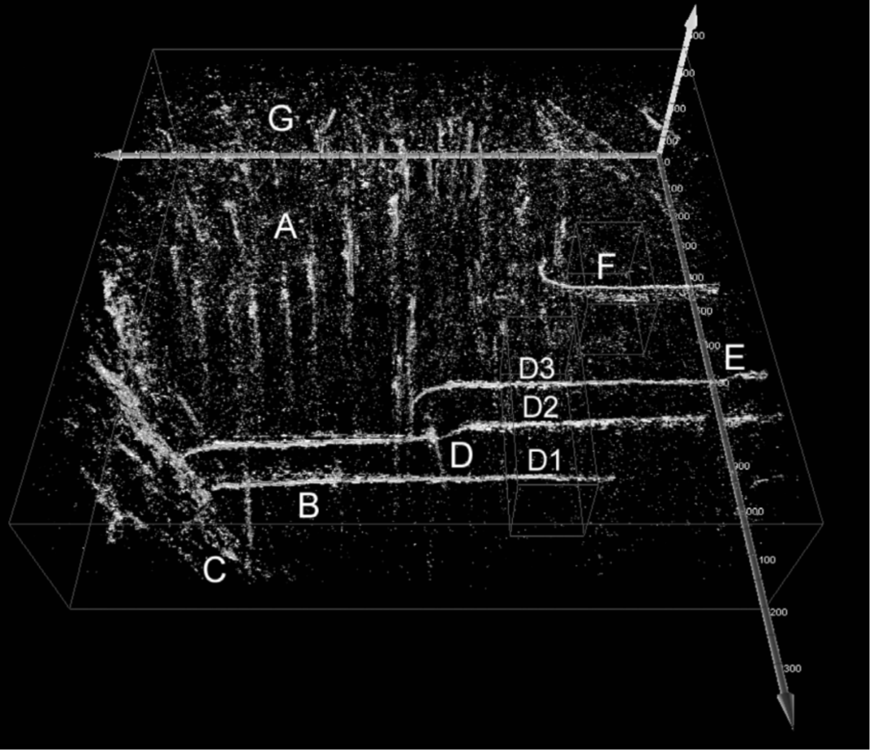

転位線のコントラストの基本的解釈

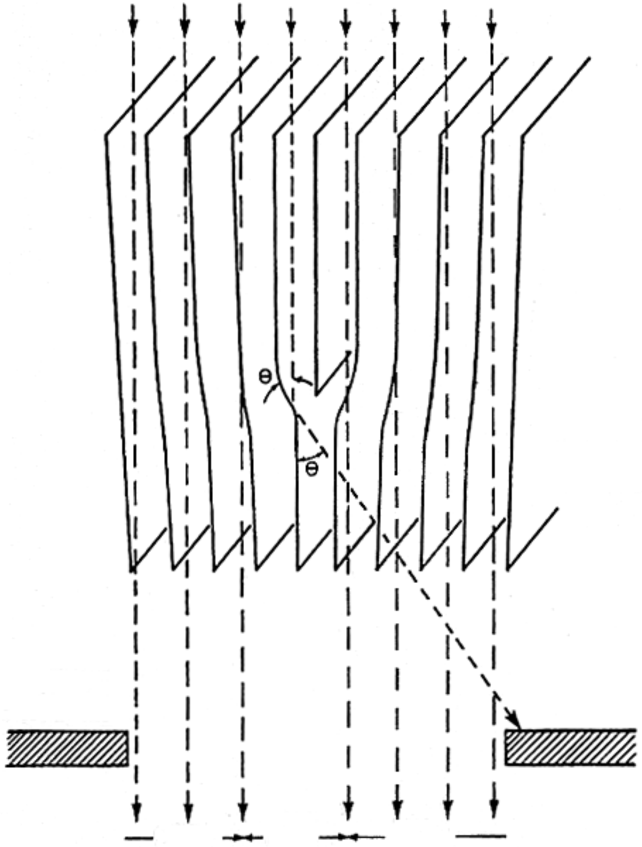

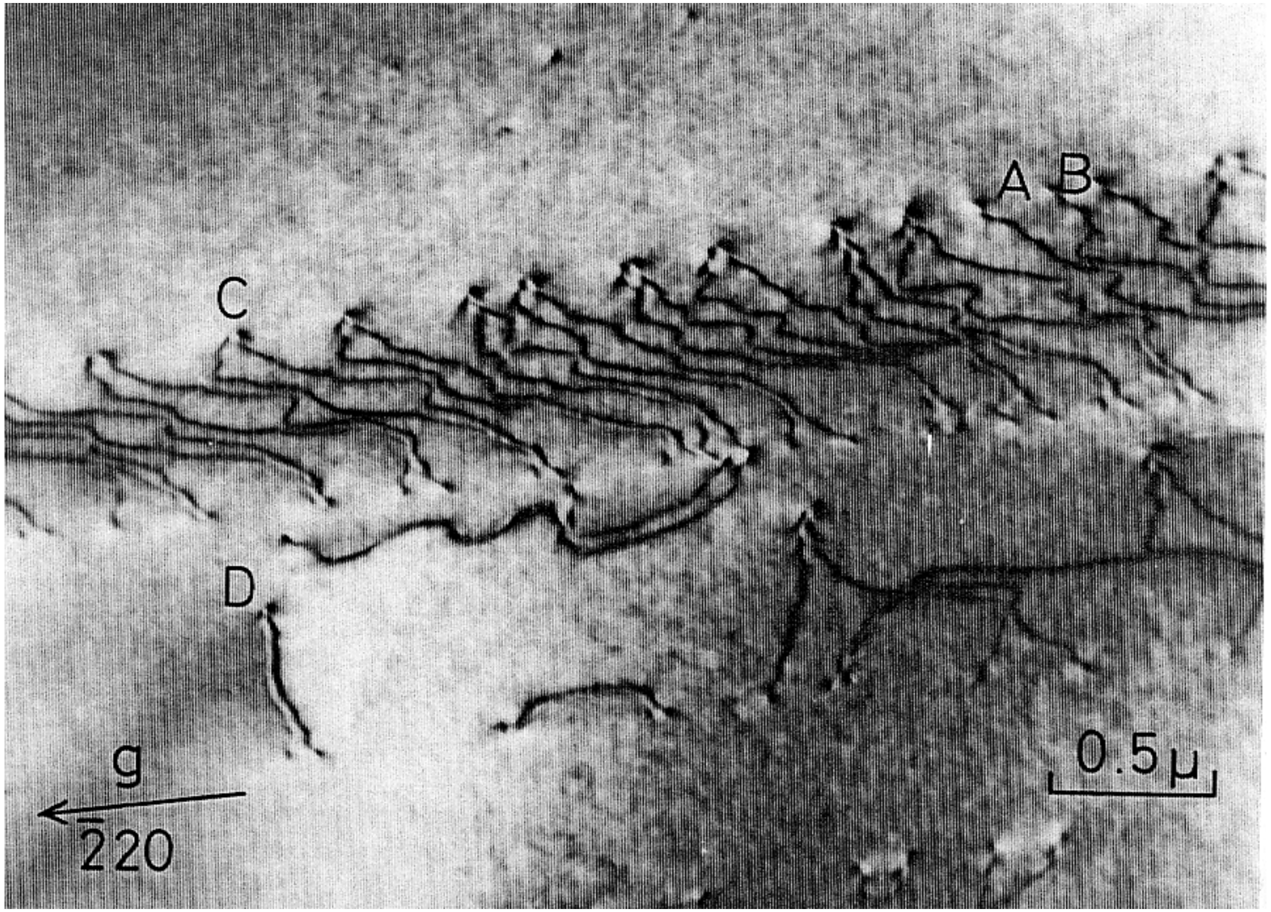

転位：線状欠陥

格子面が湾曲した転位芯近傍で

Bragg 反射した波が絞りでカットされる

↓

明視野像で転位線が暗線となって見える

Courtesy of
Prof.
Tomokiyo

3D diffraction contrast imaging:
keep a diffraction condition during specimen tilt.

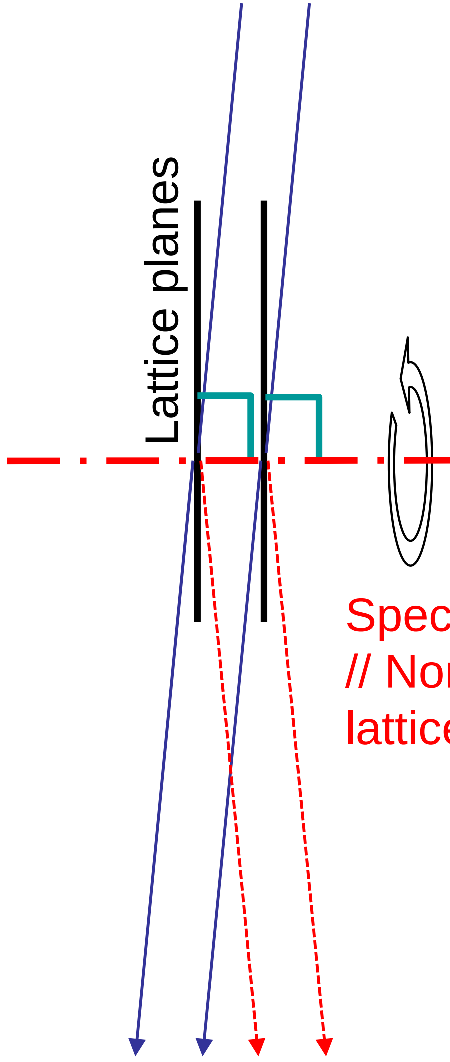

High-angle single-tilt
tomography holder
(Fischione™)

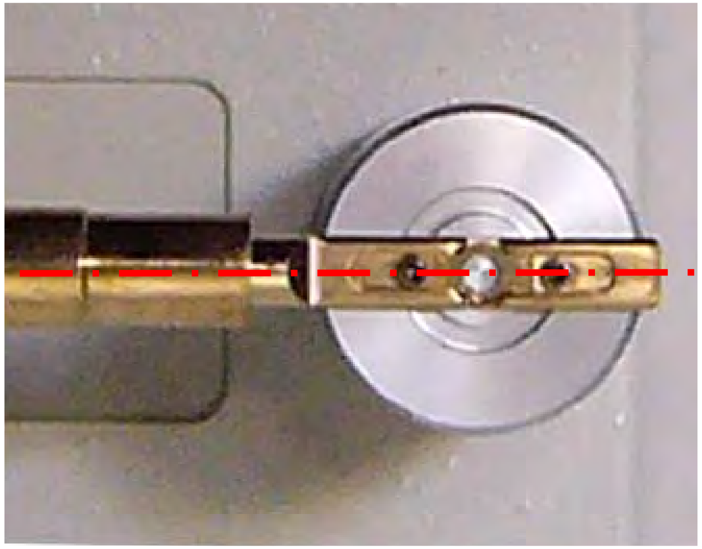

Diffraction pattern in
a two-beam condition

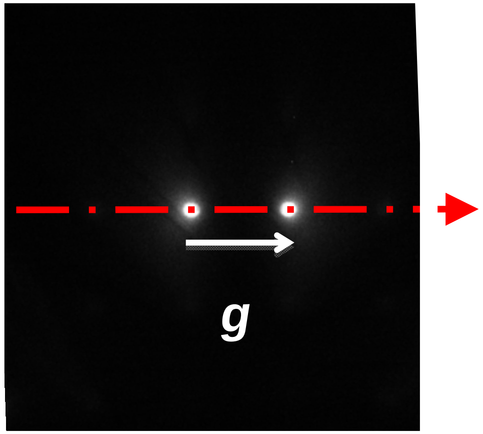

In order to keep the diffraction condition during specimen tilt,

Well-controlled sample preparation (almost by chance)

Incident beam-tilt (causes image distortion due to aberration)

Double-tilt tomography holder (not commercially available)

We developed a high-angle triple-axis (HATA) specimen holder.

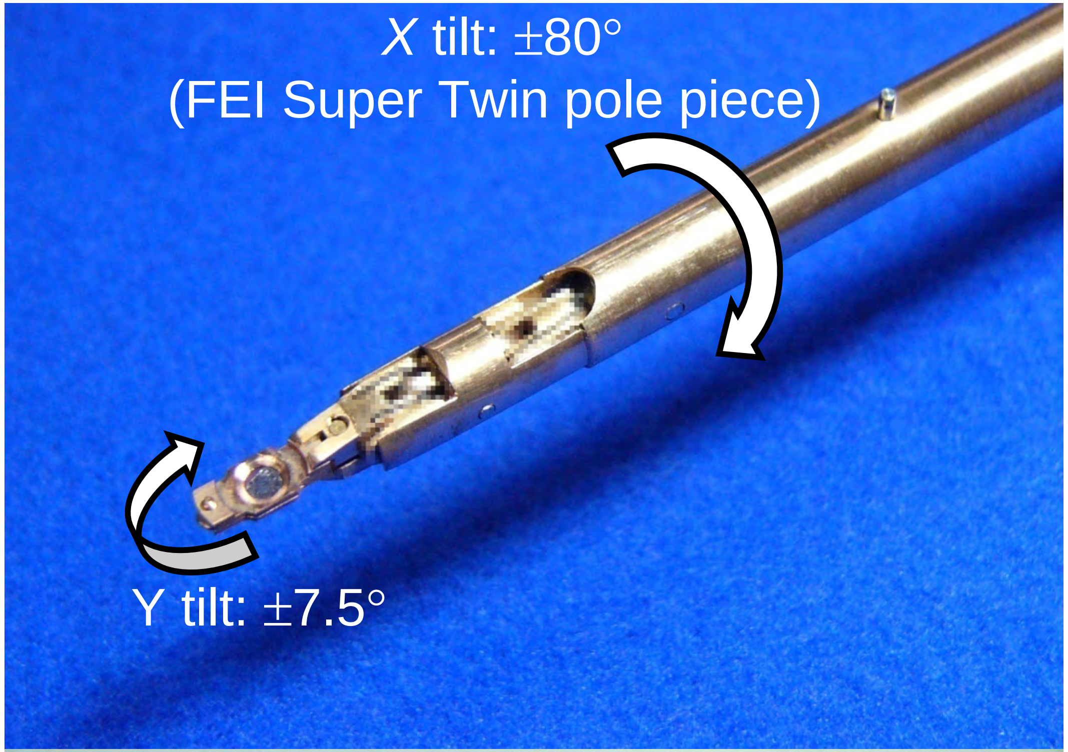

X tilt: ±80°
(FEI Super Twin pole piece)

Y tilt: ±7.5°

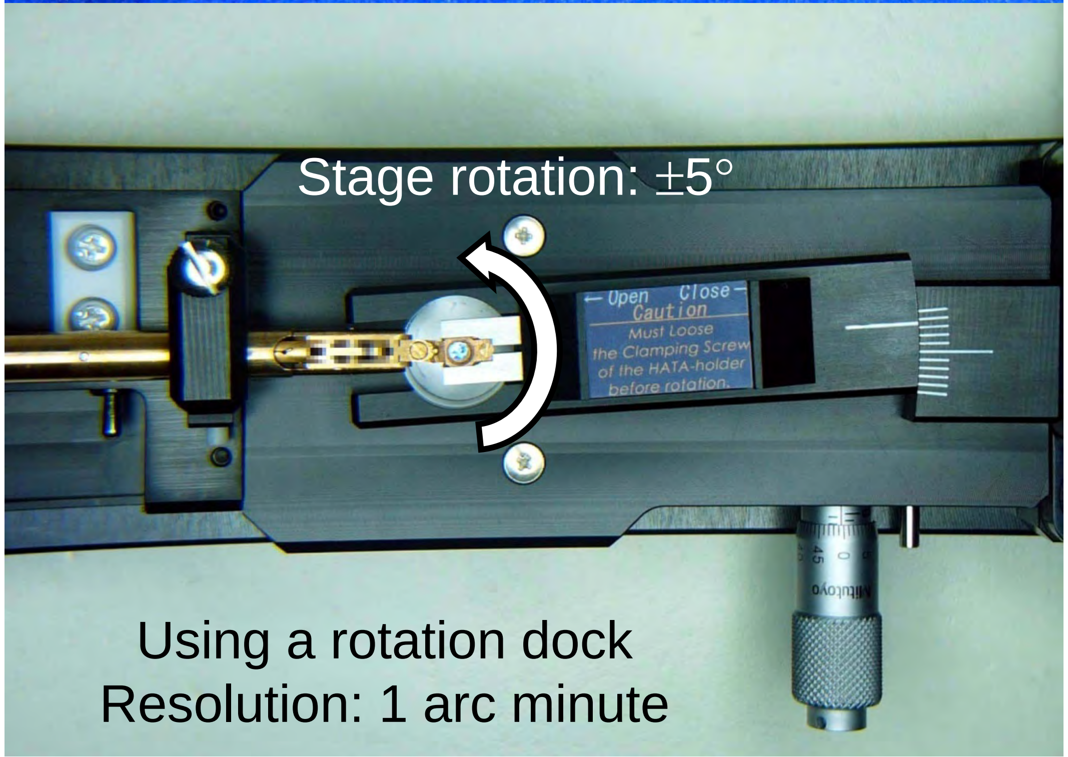

Stage rotation: ±5°

Using a rotation dock
Resolution: 1 arc minute

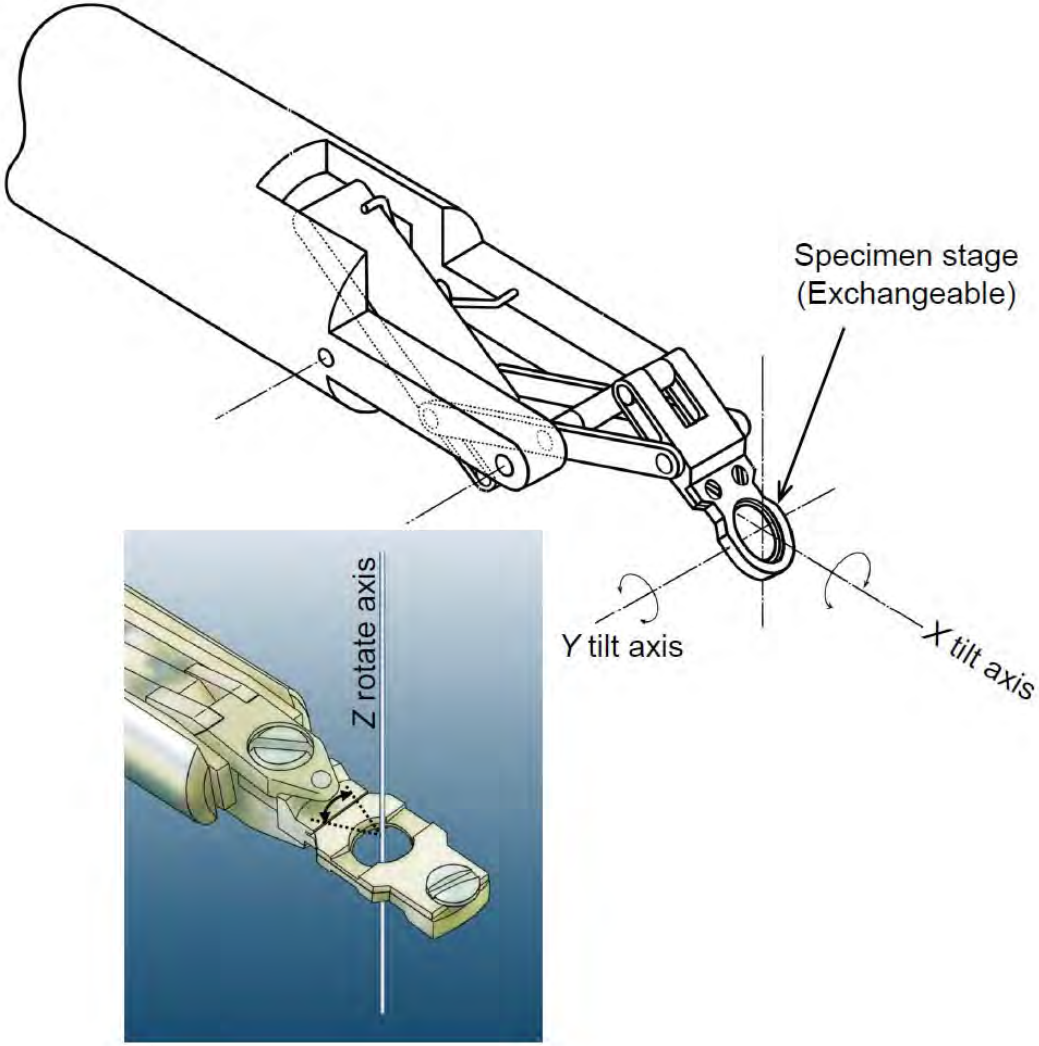

http://www.melbuild.com/
Hata *et al.* submitted

TEM (transmission electron microscopy) and STEM (scanning TEM)

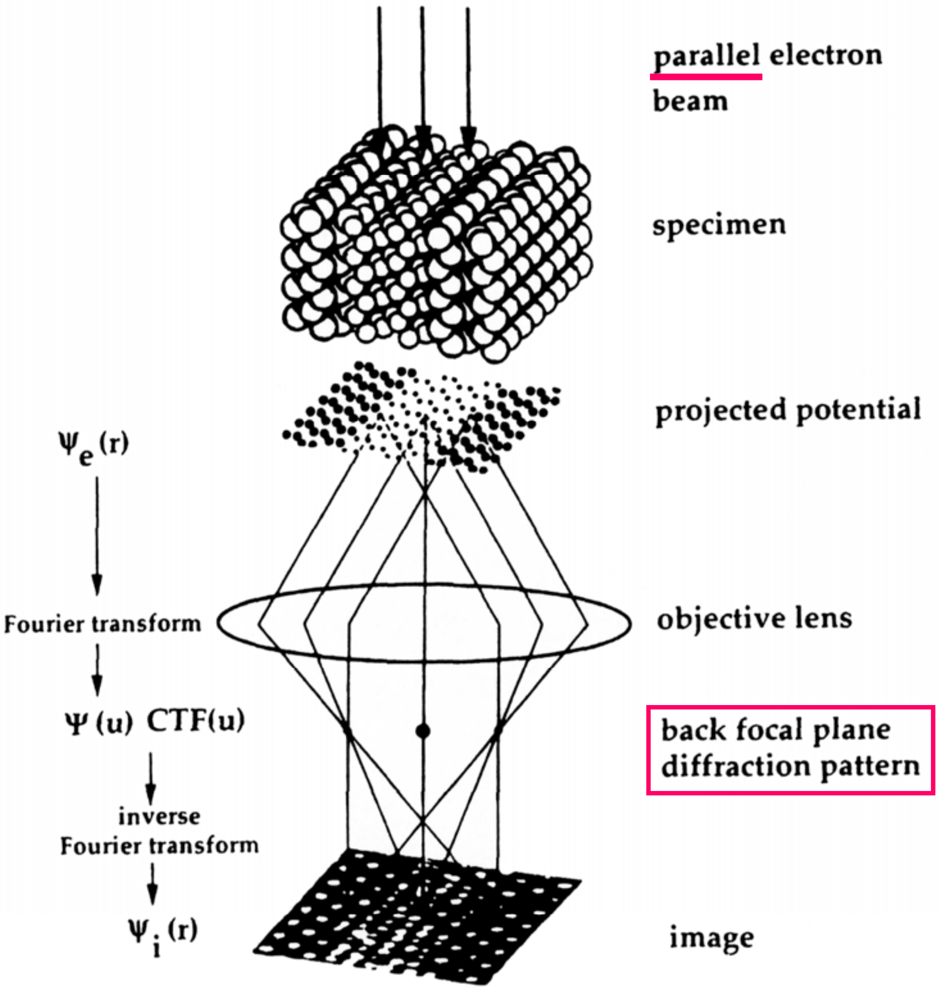

Fig. 1 Schematic of the imaging process in a high-resolution electron microscope.

電子回折図形
（散乱角度分布）

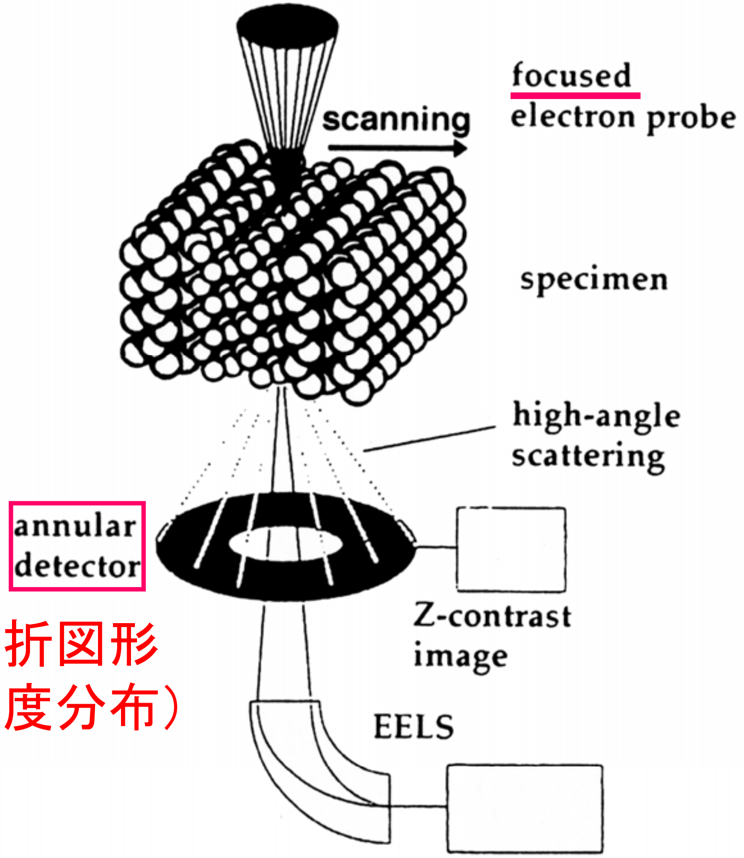

Fig. 8 Schematic of incoherent STEM-imaging using a high-angle annular dark field detector. Simultaneously bright-field imaging or electron energy loss spectroscopy is possible.

F. Phillipp: *Mater. Trans., JIM*, **39** (1998), 888.

STEM imaging modes

Fe-3 mass% Cu alloy

Bright field | Low-angle annular dark-field | High-Angle ADF

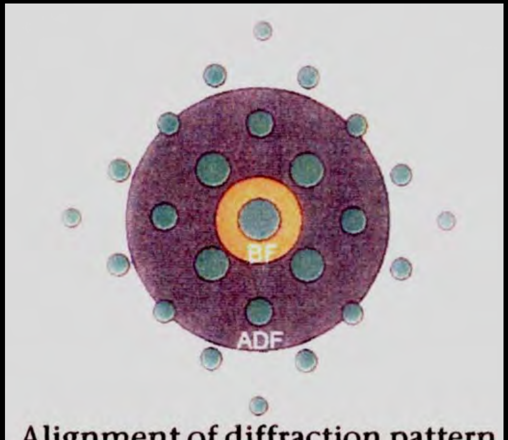

Alignment of diffraction pattern on BF/DF

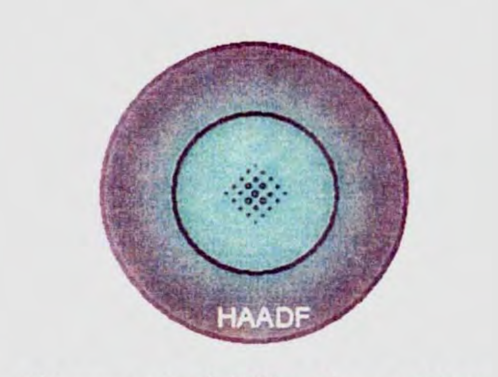

Alignment of diffraction pattern on HAADF

Courtesy of Profs. Tsuchiyama, Takaki (Kyushu U.) and FEI

Influence of deviations from Bragg conditions

Dislocations in bcc ferrite (α-Fe)

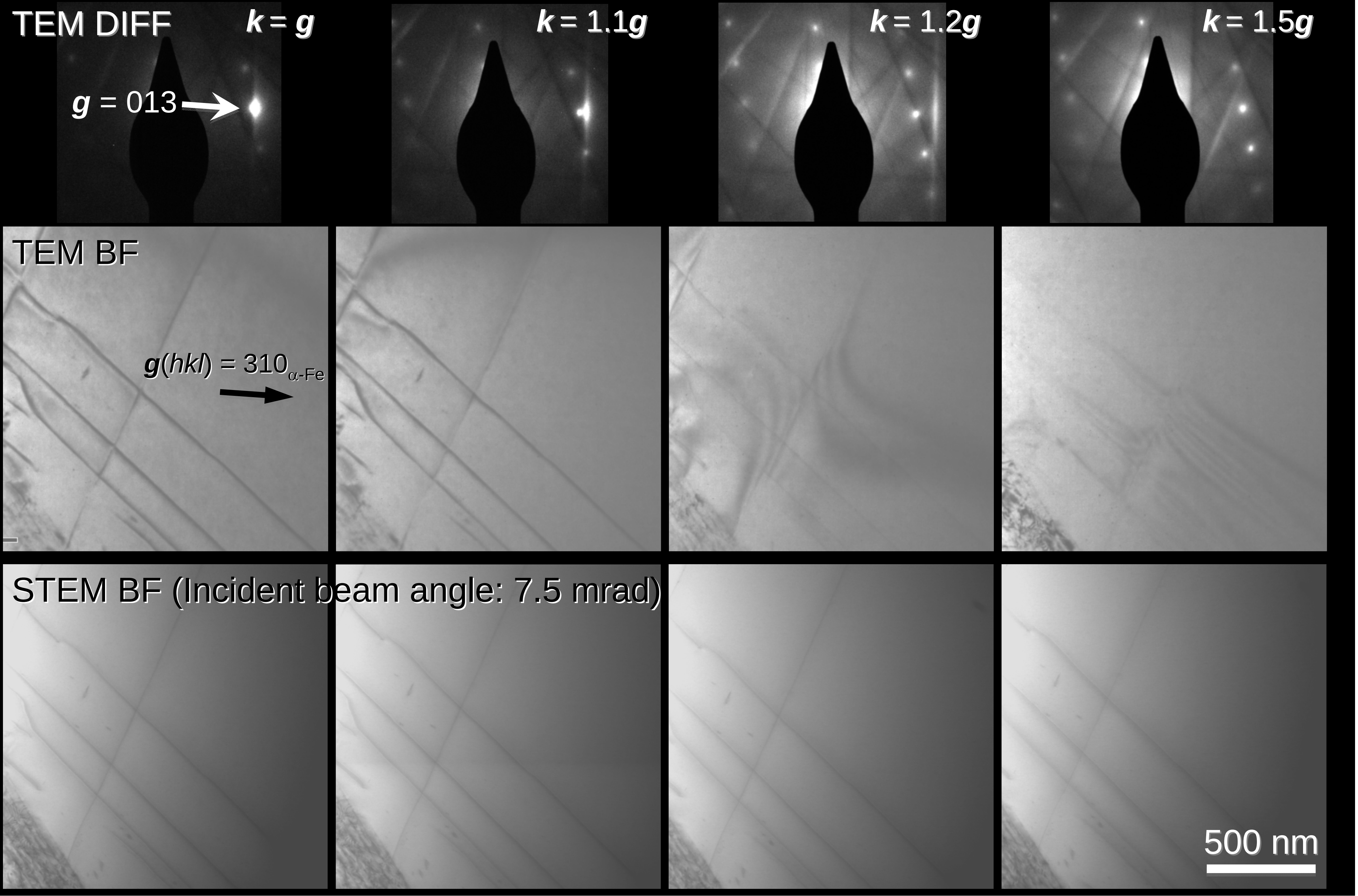

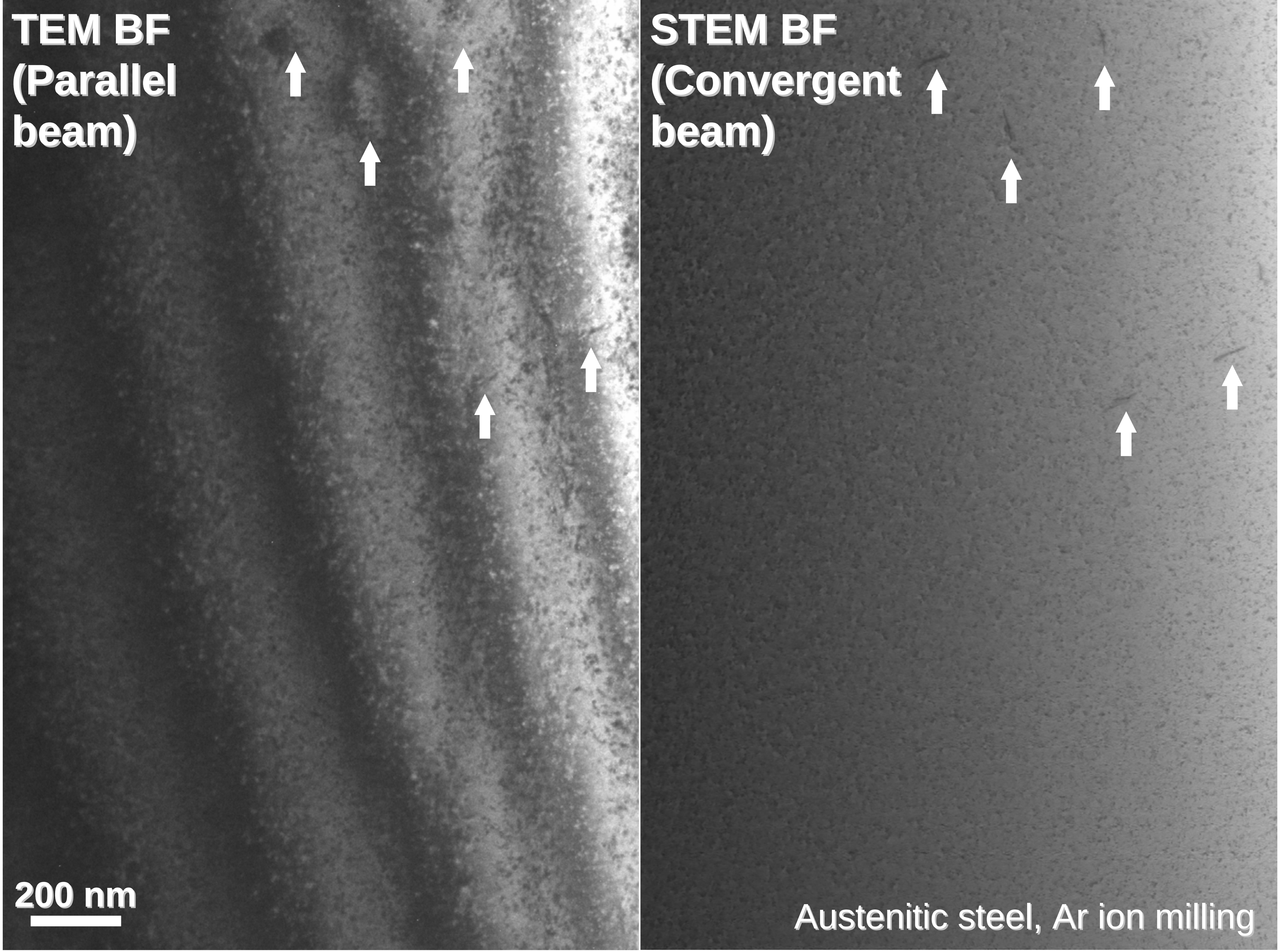
TEM BF
(Parallel
beam)
STEM BF
(Convergent
beam)
200 nm
Austenitic steel, Ar ion milling

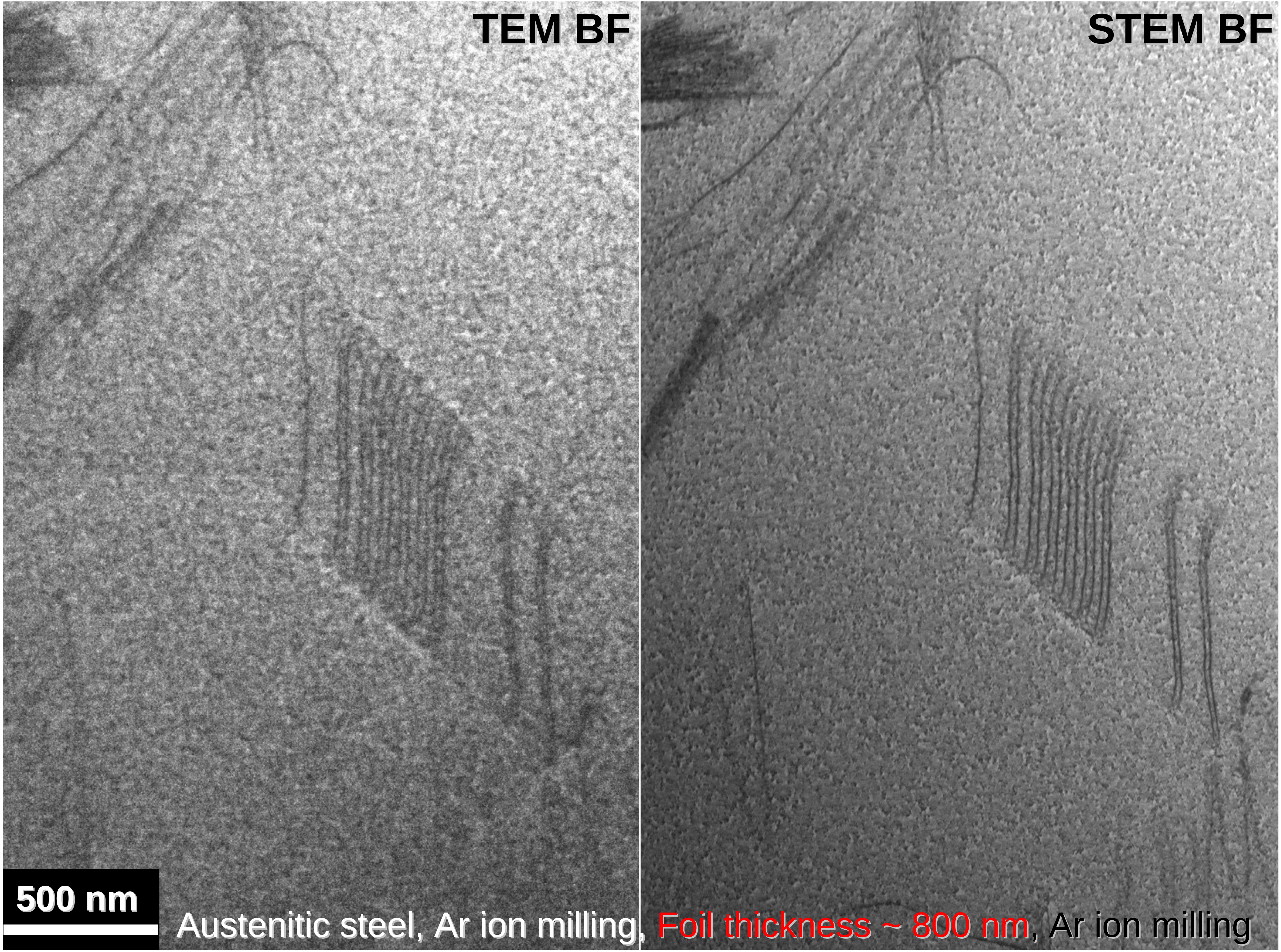

Austenitic steel, Ar ion milling, Foil thickness ~ 800 nm, Ar ion milling

STEM dislocation images with different *g* vectors

Austenitic steel with FCC structure

b = <110>*a*/2 (perfect dislocation) or <112>*a*/6 (partial dislocation)

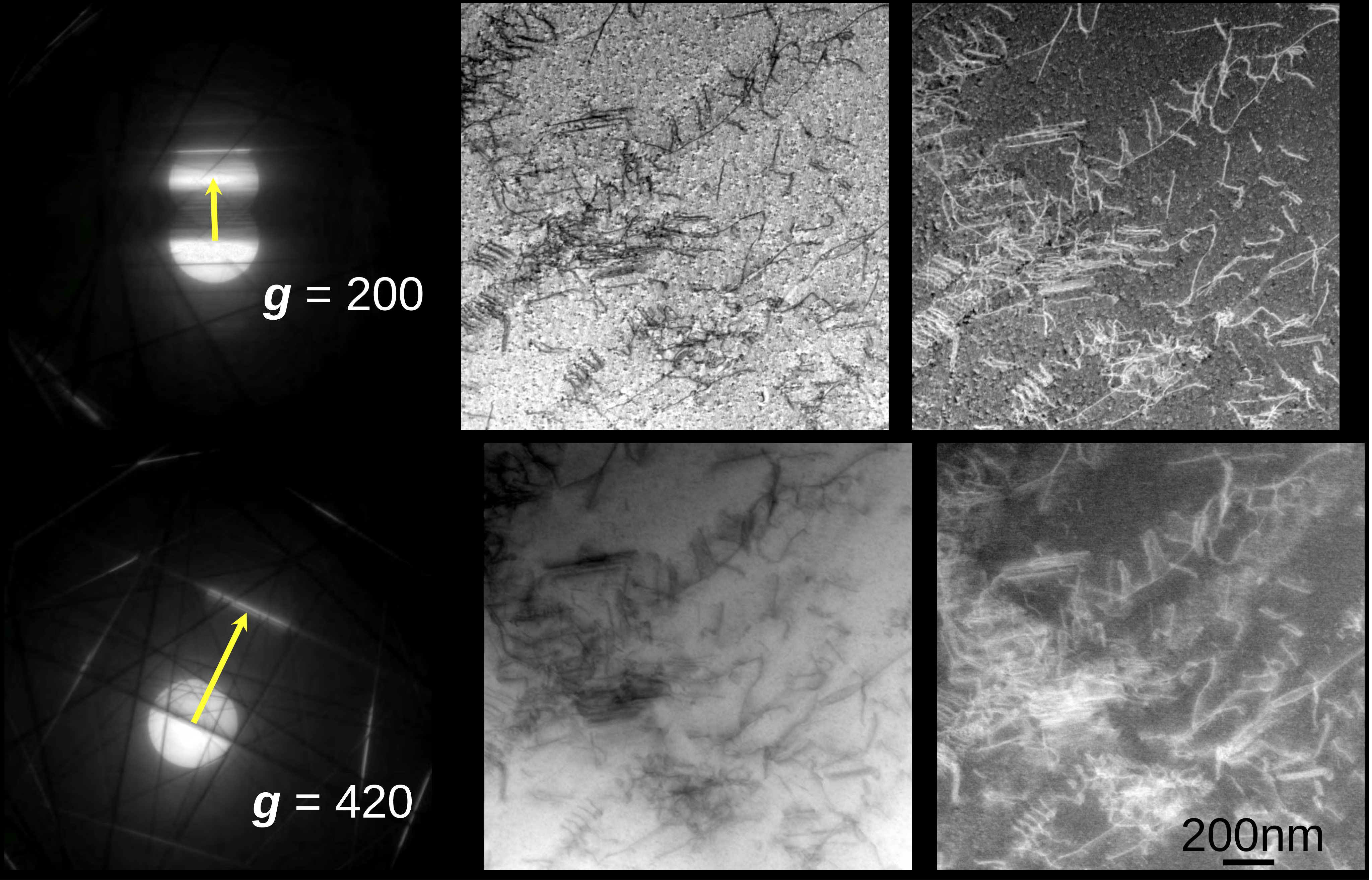

Keep two-beam condition (STEM mode)

Austenitic (fcc) steel

Diffraction condition
K = ***g***(200)

Specimen-tilt angle
-70° ~ +70°

Misorientation angle
between
specimen-tilt axis
and ***g***(200) < 1°

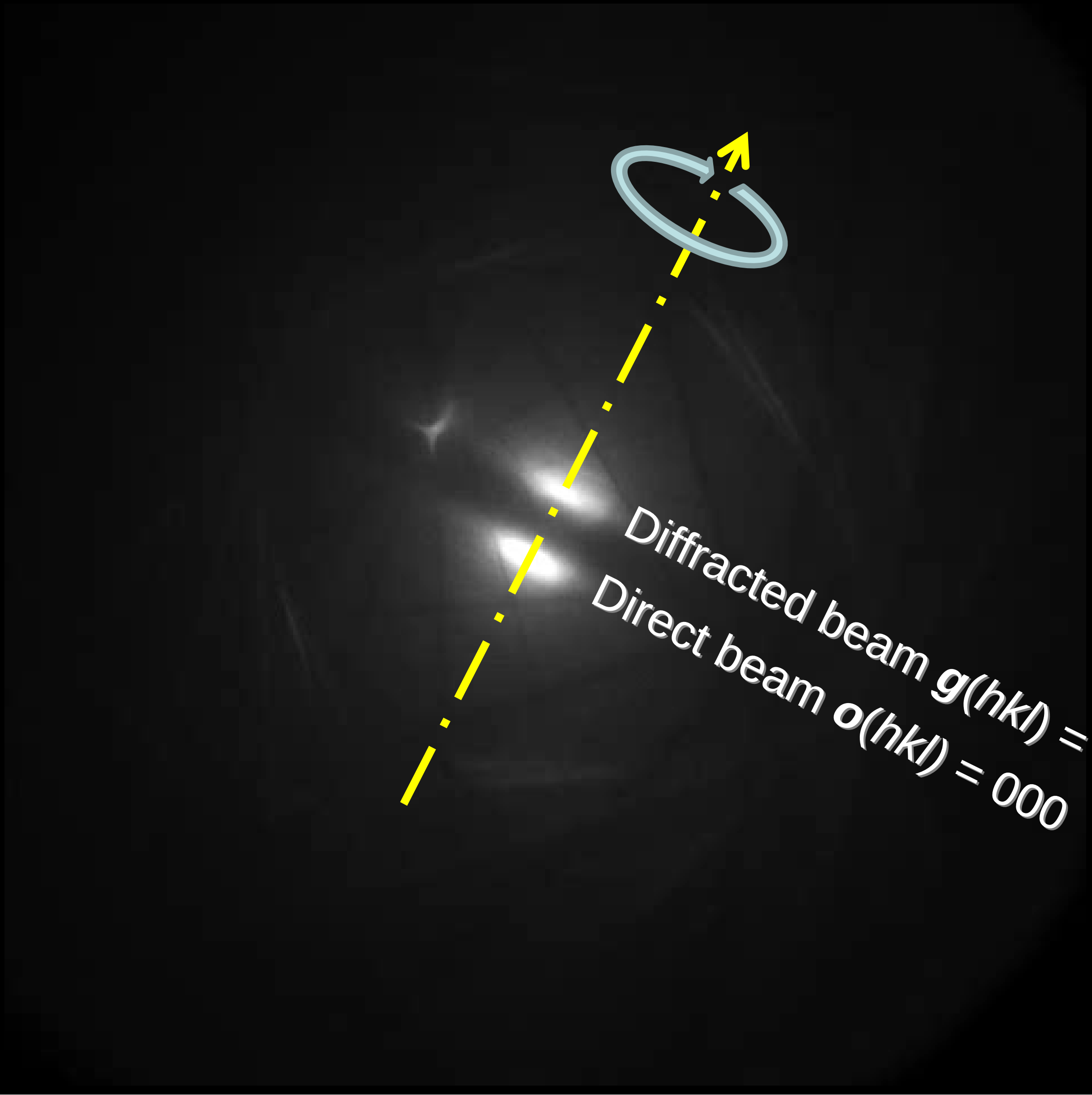

Diffracted beam ***g***(*hkl*) = 200
Direct beam ***o***(*hkl*) = 000

STEM tilt series of dislocations

SUS316 after 5% compressive deformation at room temperature

STEM BF tilt series
（Contrast reversal）

Specimen-tilt angle
-70° ~ +70°

HATA holder

Specimen-tilt axis //
$\boldsymbol{g}(hkl) = 200_{\mathrm{fcc}}$

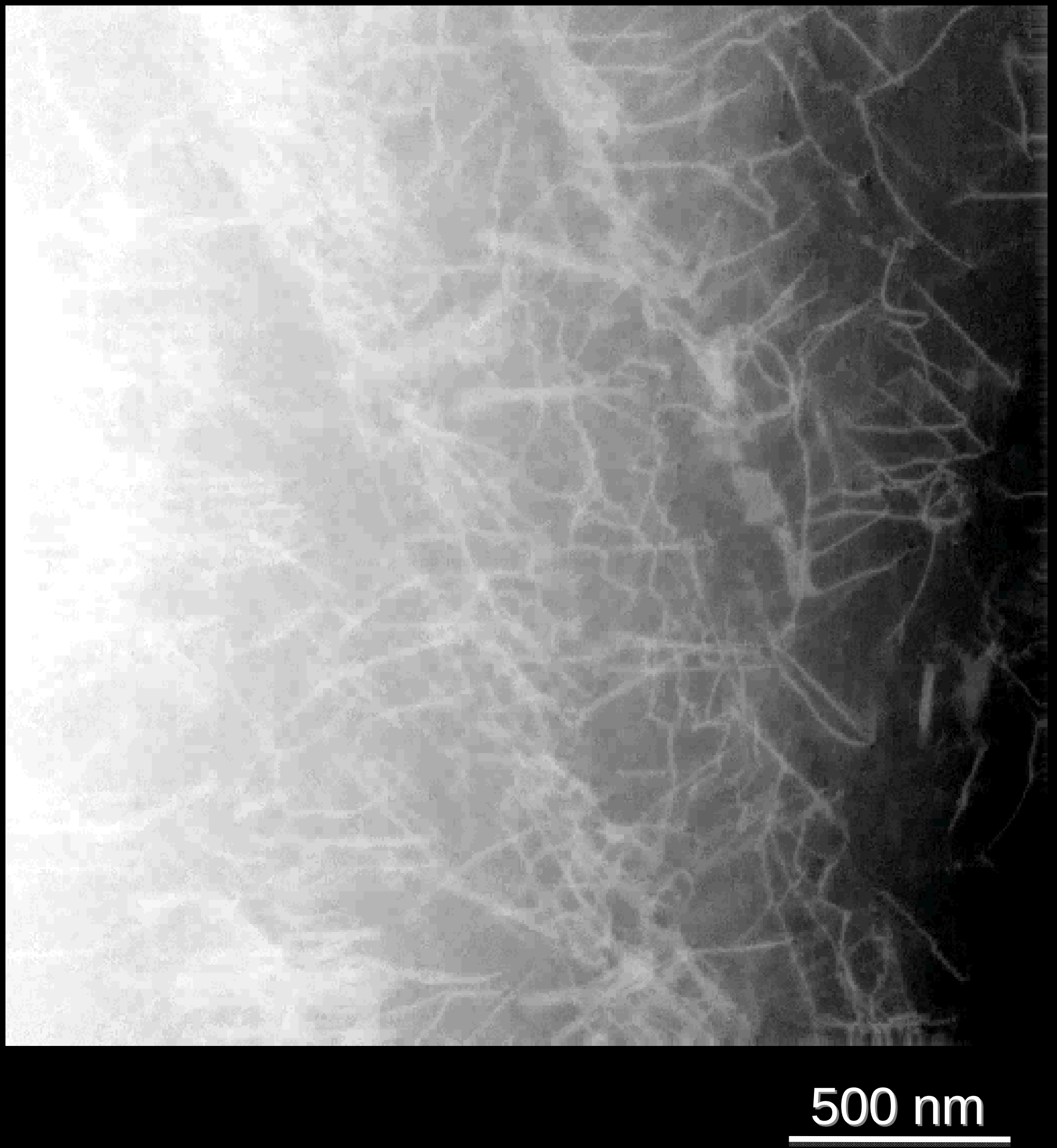

3D reconstruction of dislocations

SUS316 after 5% compressive deformation at room temperature

Complete visualization of dislocation arrangements by dual-axis tomography

(Austenitic steel)

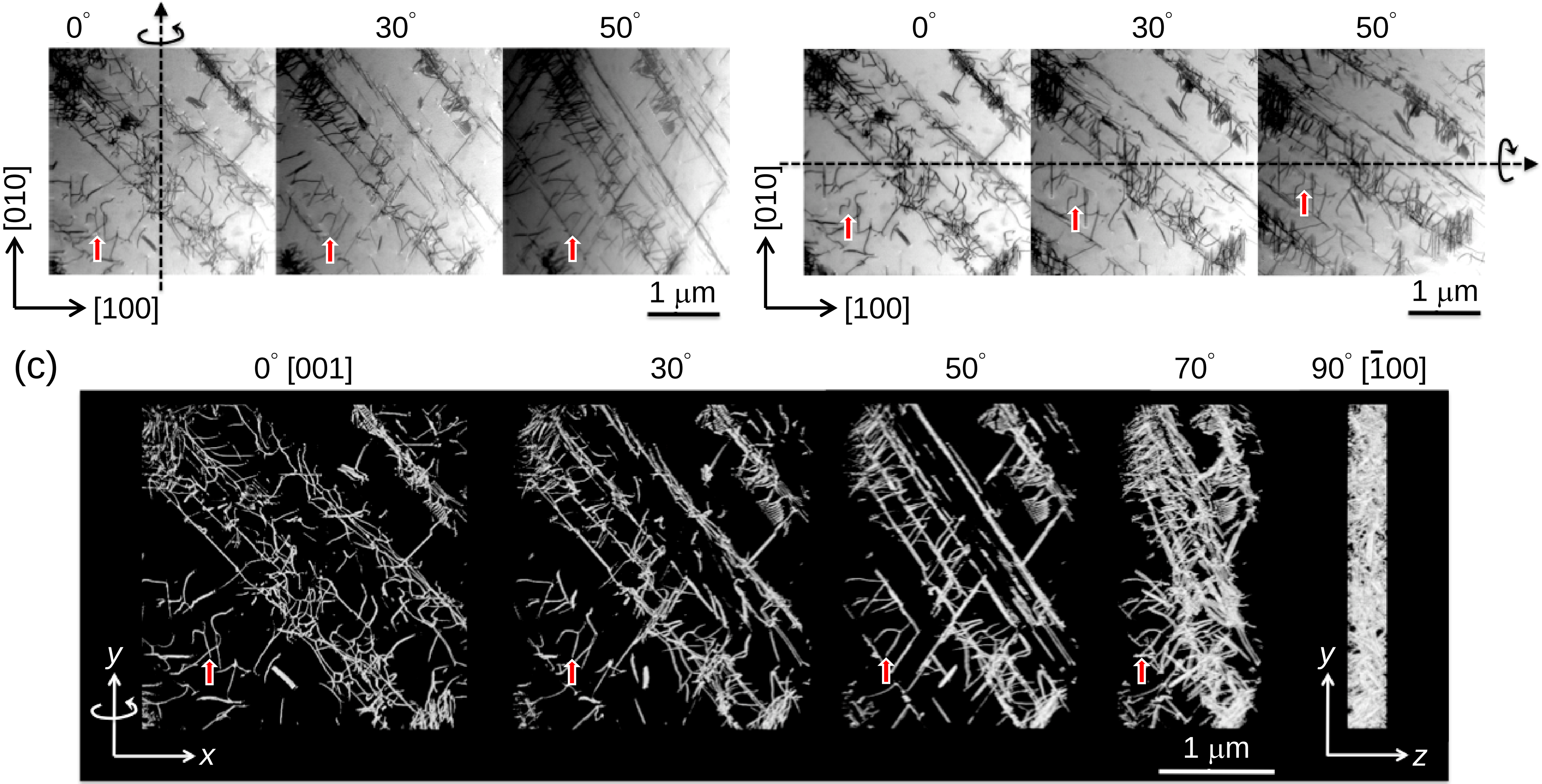

(a) Specimen-tilt axis parallel to $\boldsymbol{g}_1(hkl) = 020_{\mathrm{FCC}}$

(b) Specimen-tilt axis parallel to $\boldsymbol{g}_2(hkl) = 200_{\mathrm{FCC}}$

(c)

$\rho = 4.0 \times 10^{13}\ \mathrm{m}^{-2}$

Number of dislocations in 2D tomograms

SUS, 3% strained at R. T.

Reconstructed 3D volume **(1 pixel = 3 nm)**

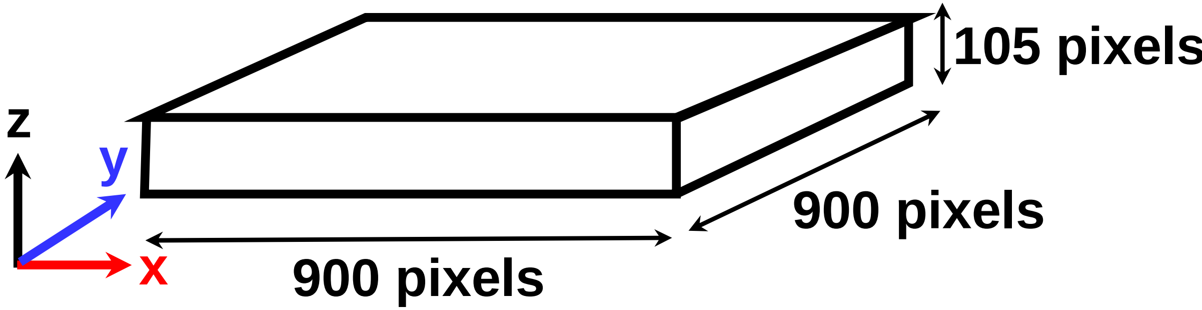

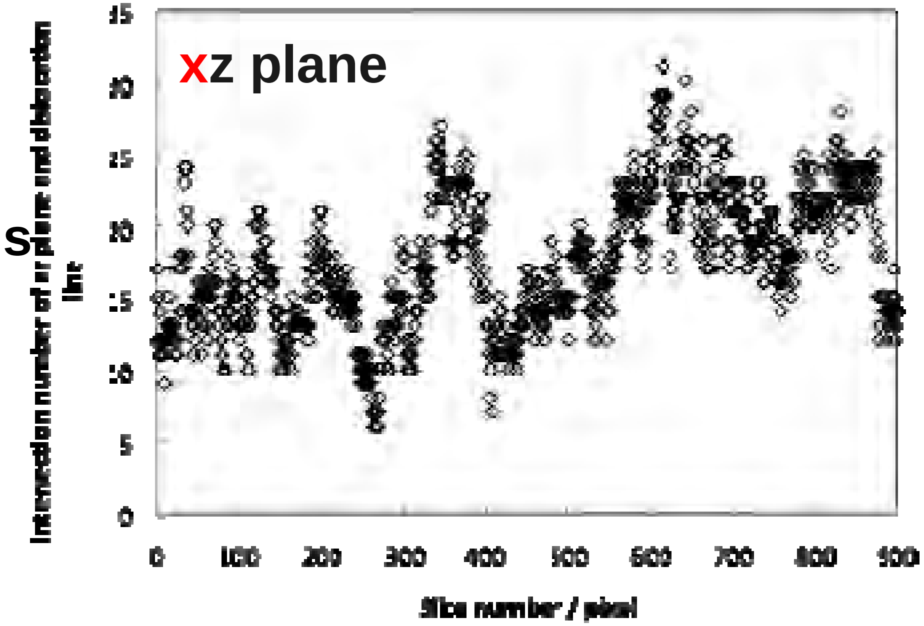

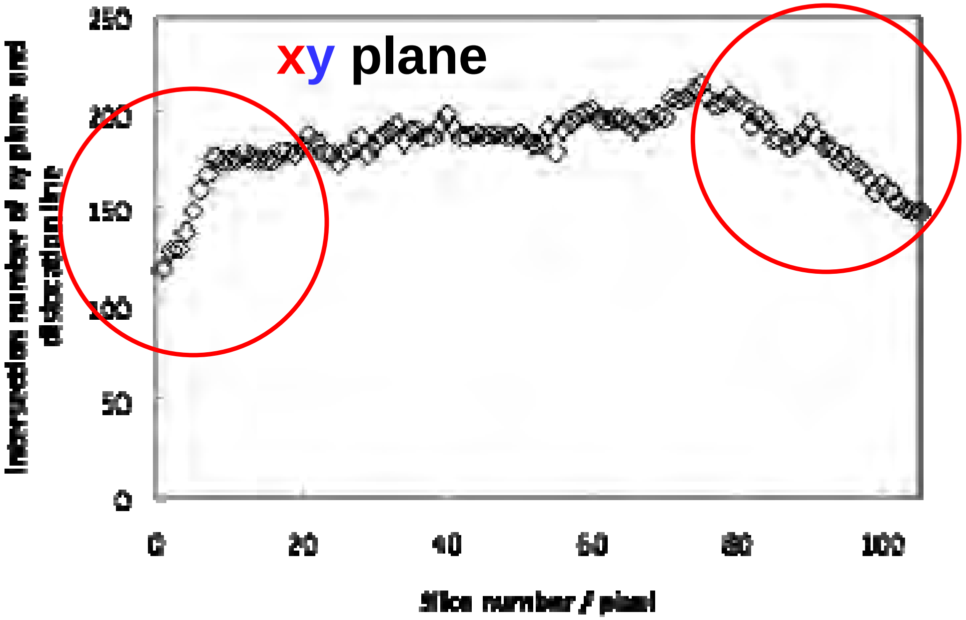

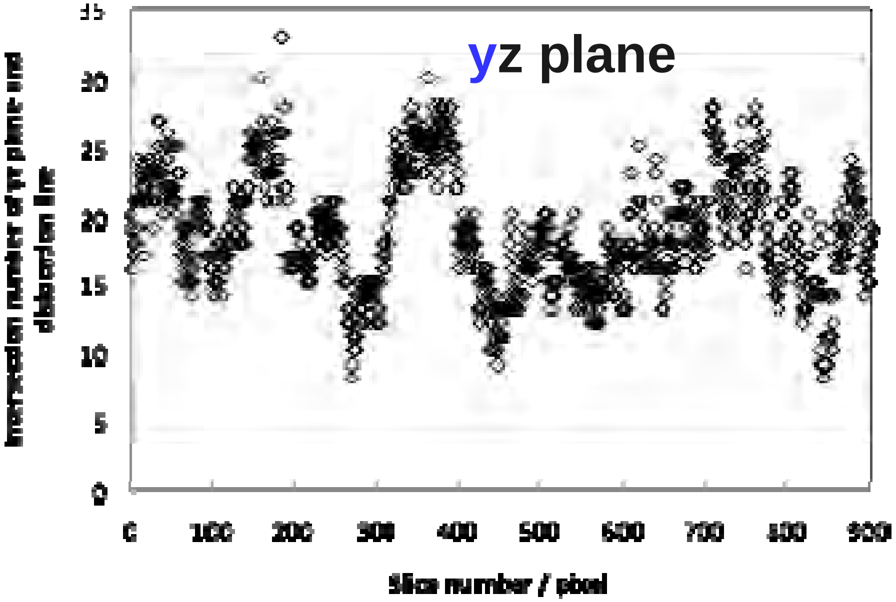

20-30% reduction of dislocation density near the specimen surface

Dislocation density evaluated from 2D image and 3D volume

Austenitic steel, 10% compressive deformation at R. T.

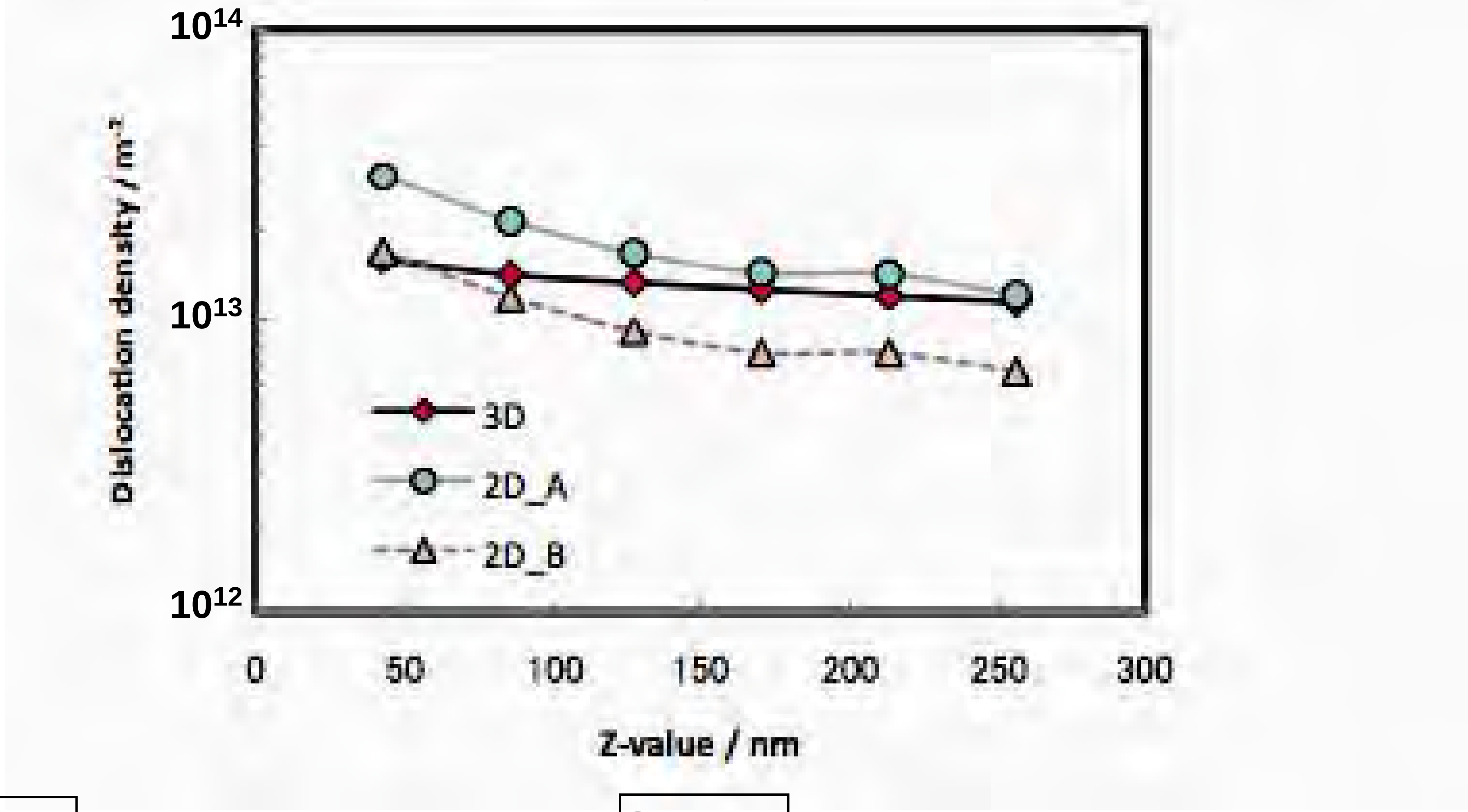

2D_A

$$\rho = \frac{2N}{Lt}$$

L: total length of straight lines on 2D image
N: intersection number of straight lines and dislocations
t: specimen thickness

2D_B

$$\rho = \left(\frac{n_1}{L_1} + \frac{n_2}{L_2} \right) \frac{1}{t}$$

L_1: total length of vertical lines
n_1: intersection number of vertical lines and dislocations
L_2: total length of horizontal lines
n_2: intersection number of horizontal lines and dislocations

Mitsuhara

Dislocation reconstructed under different specimen-tilt conditions

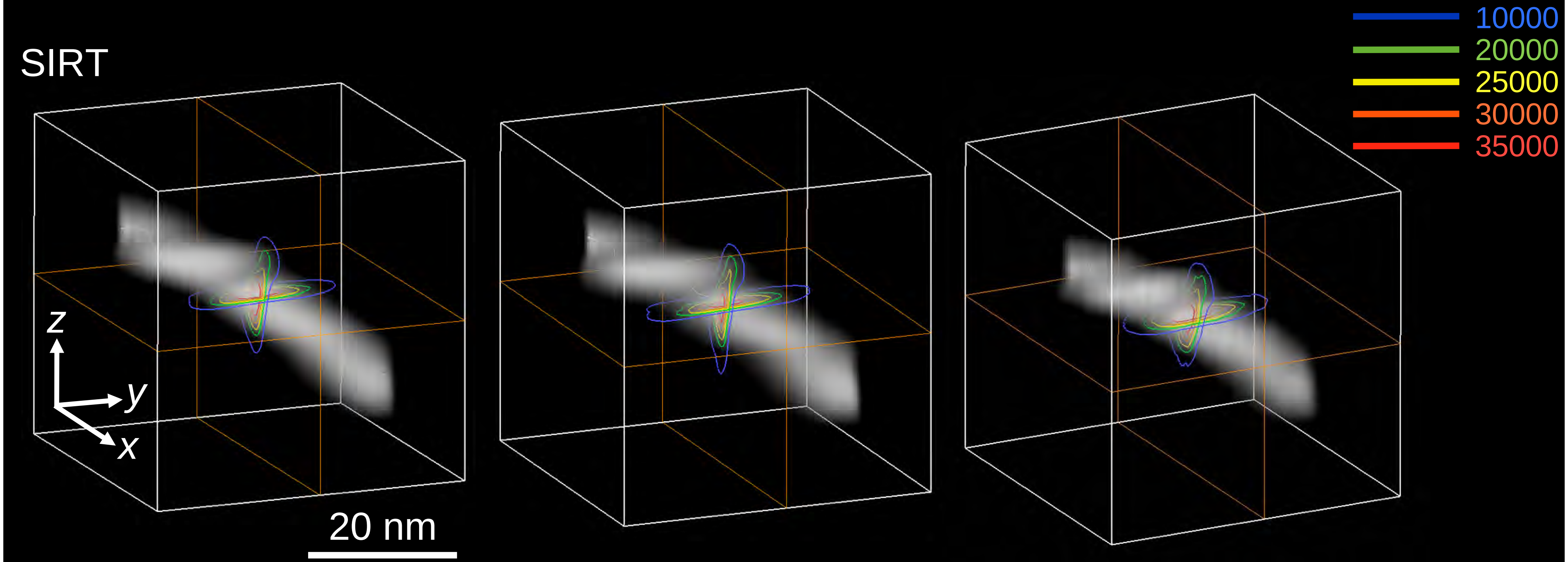

−79° to 79°, 1° step

−40° to 40°, 1° step

−70° to 70°, 10° step

Cross-sections of a reconstructed dislocation image as a function of angular range of specimen tilt

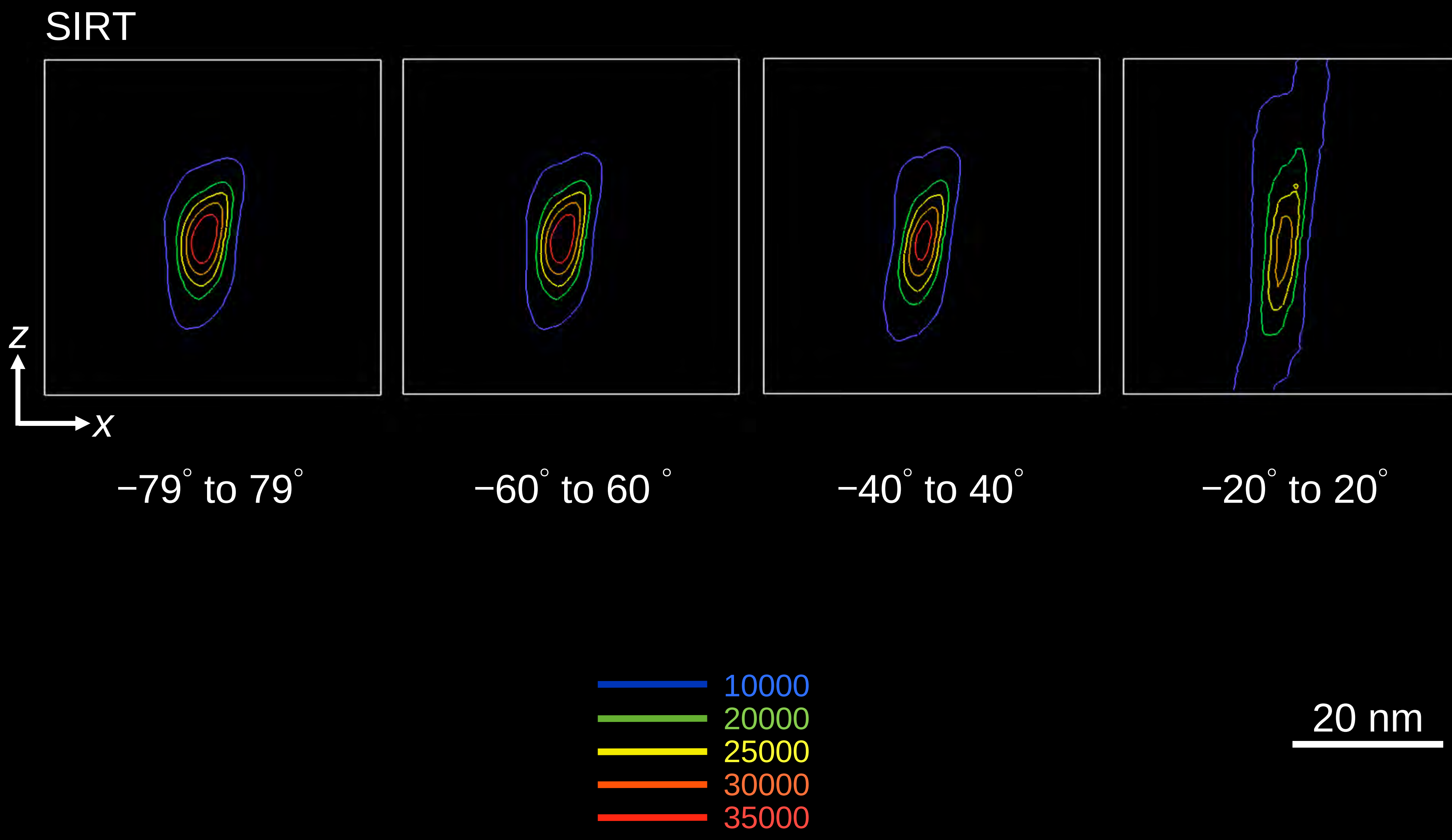

−79° to 79°

−60° to 60 °

−40° to 40°

−20° to 20°

シリコンクラック近傍の転位群のSTEMトモグラフィー観察

Vickers indent and heated at 873 K

Tanaka *et al.* Scripta Mater. (2008); J. Electron Microscopy (2010)

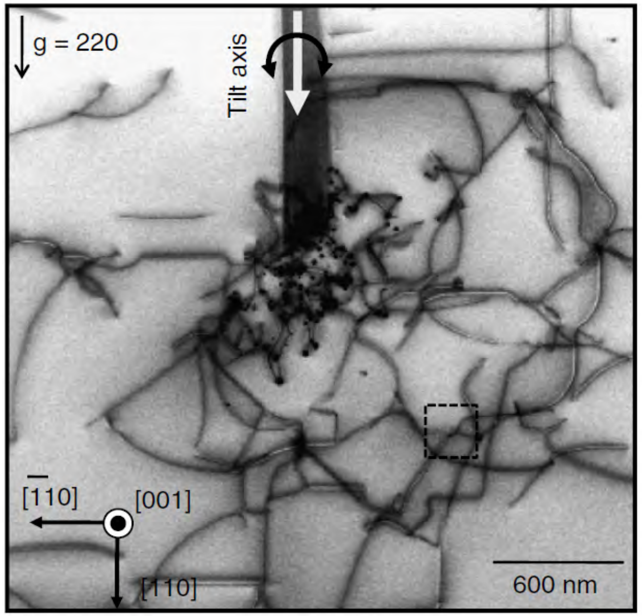

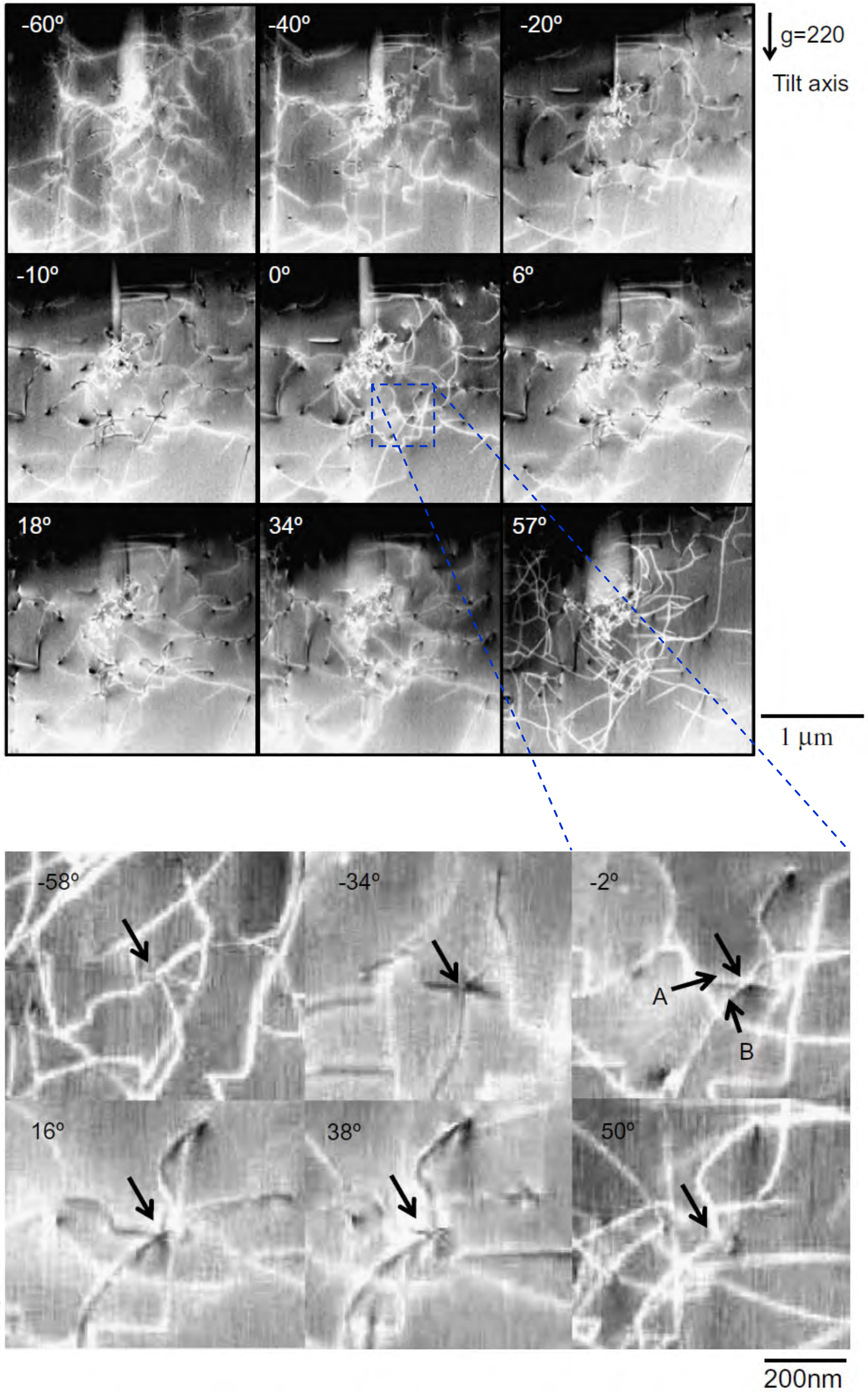

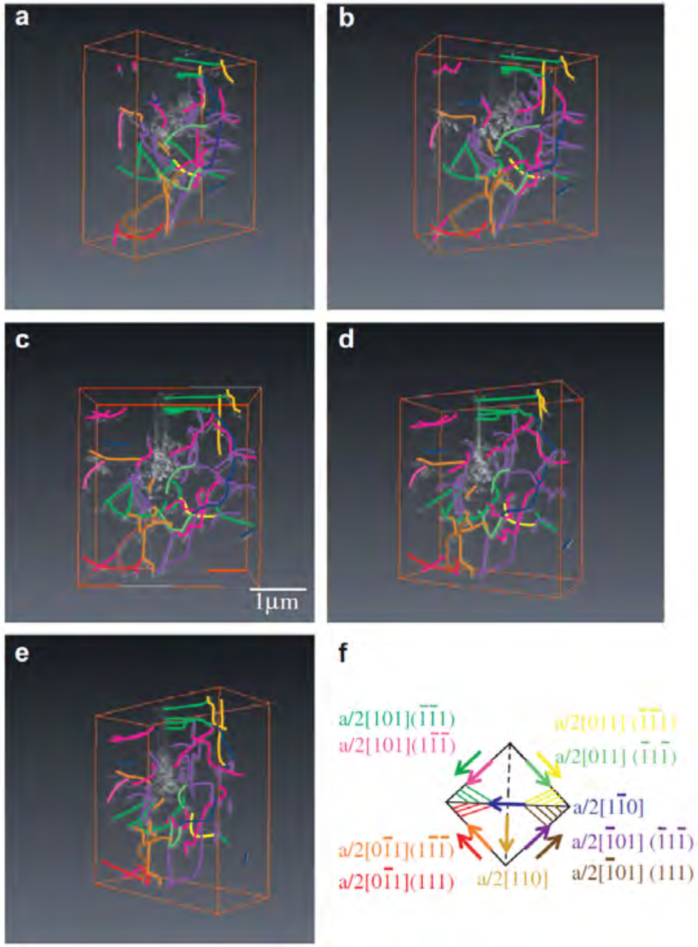

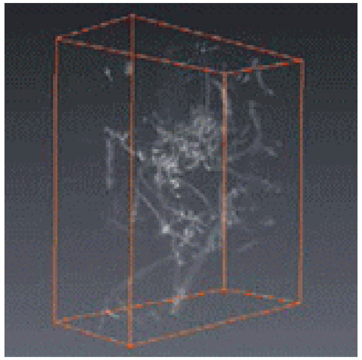

Energy-filtered HVEM JEM-1300NEF

(Installation completed in 2010, Kyushu University, Japan)

Omega type energy filter, Tomography, STEM

Penetration power of electrons as a function of accelerating voltage (assuming unity for 200 kV)

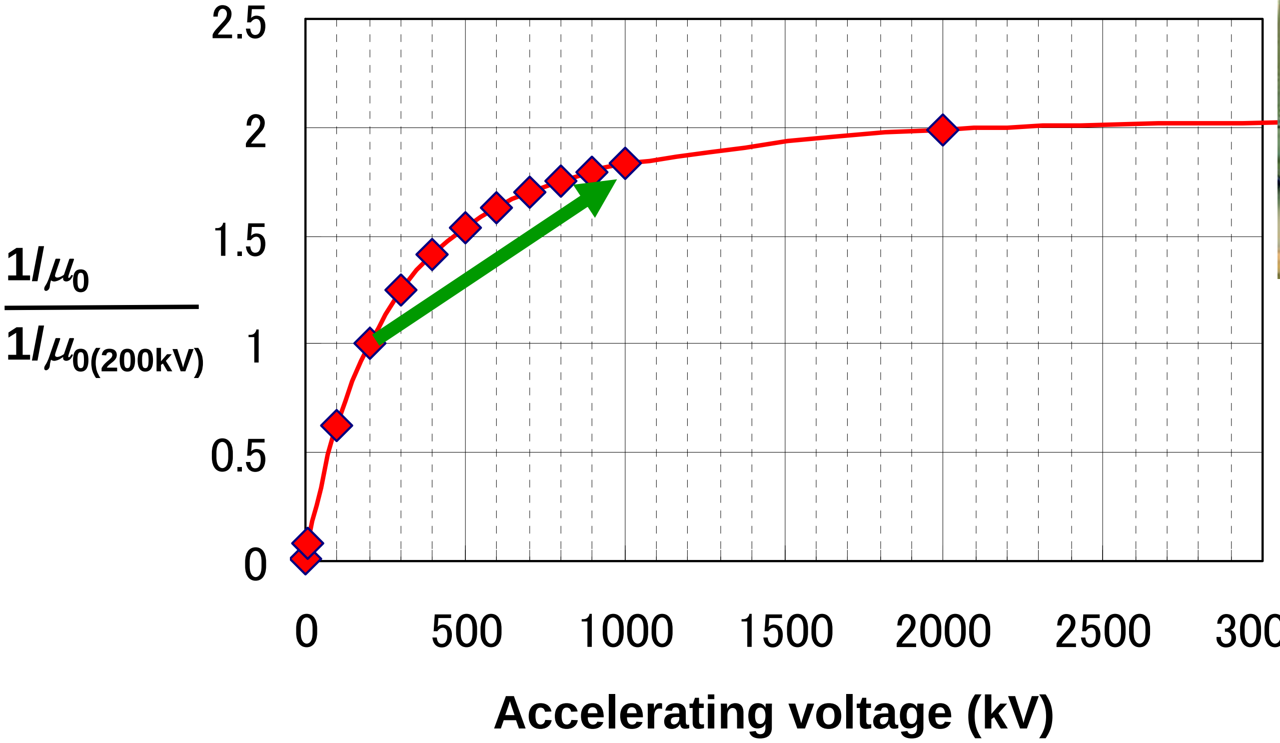

200 kV → 1000 kV
The penetration power becomes 1.8 times.

High-angle triple-axis holder for HVEM: application to thick (~3 μm) Si crystal

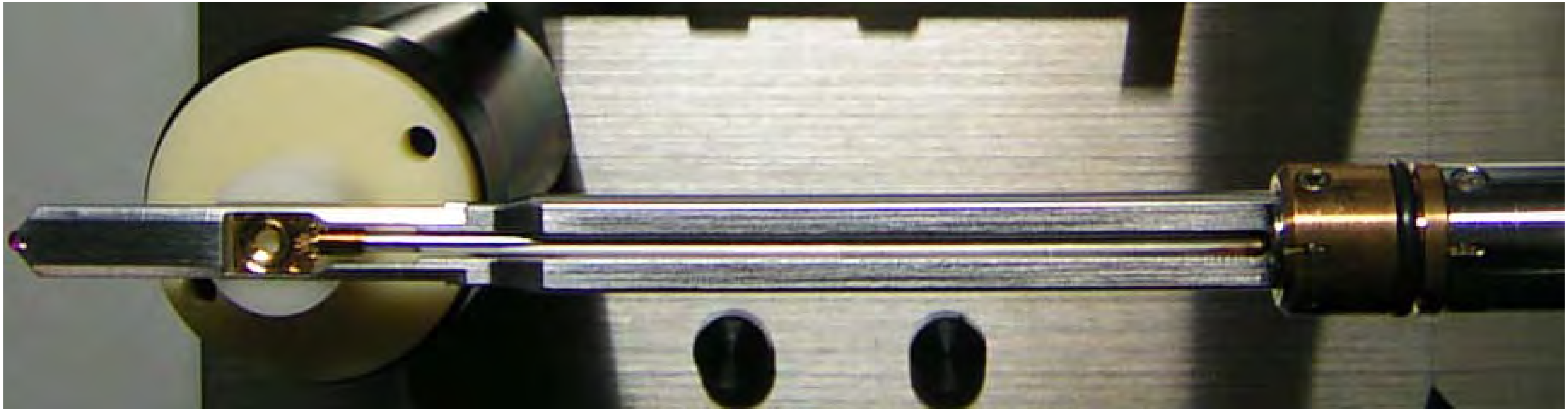

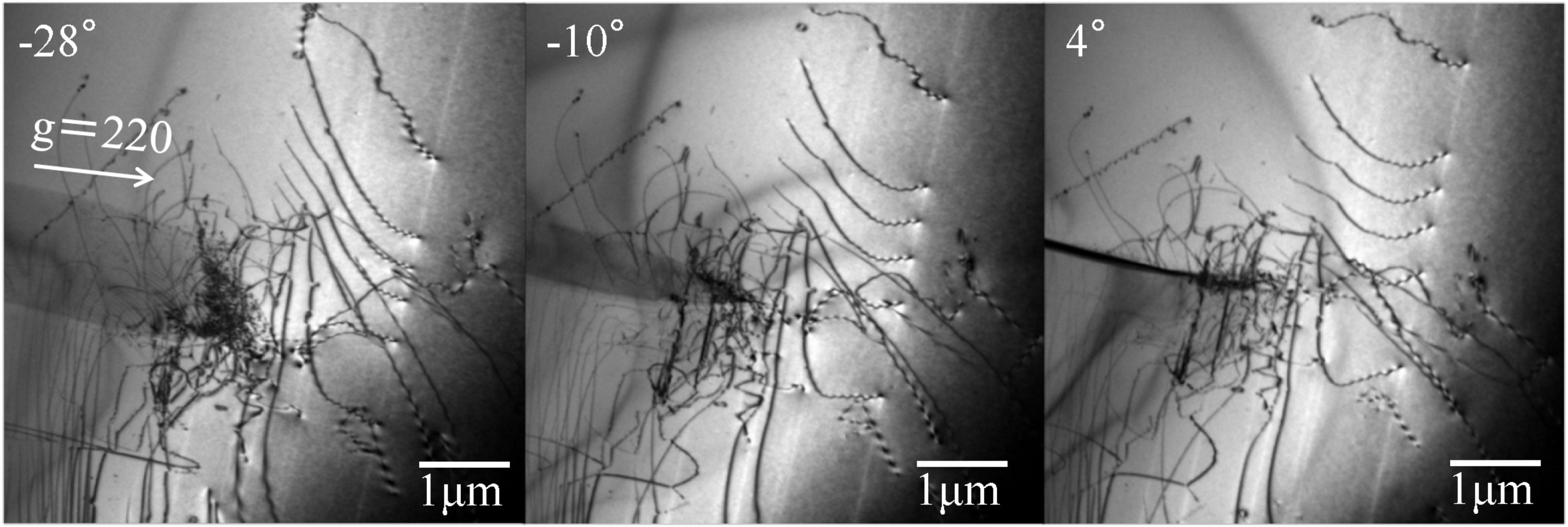

Tanaka and Higashida

Dislocation interactions and boundary formation in deformed aluminum

99.5%, d_g = 75um, 25% elongation in uniaxial tension)

Ramar *et al.* Proc. RISØ 3D/4D Symp. (2010)

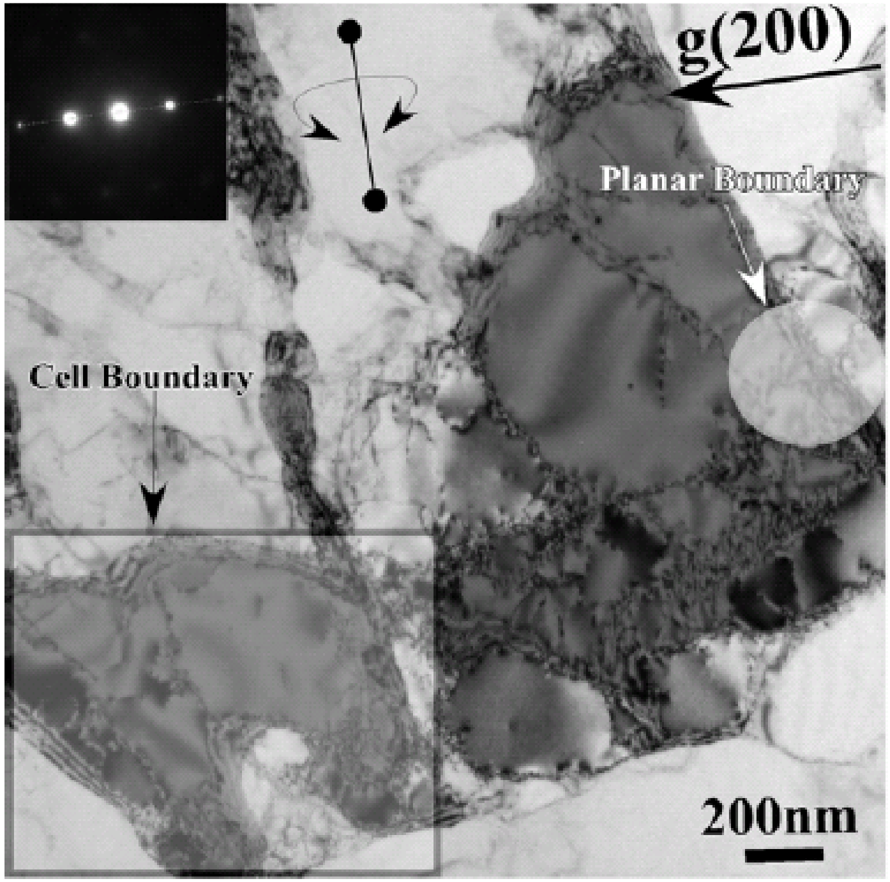

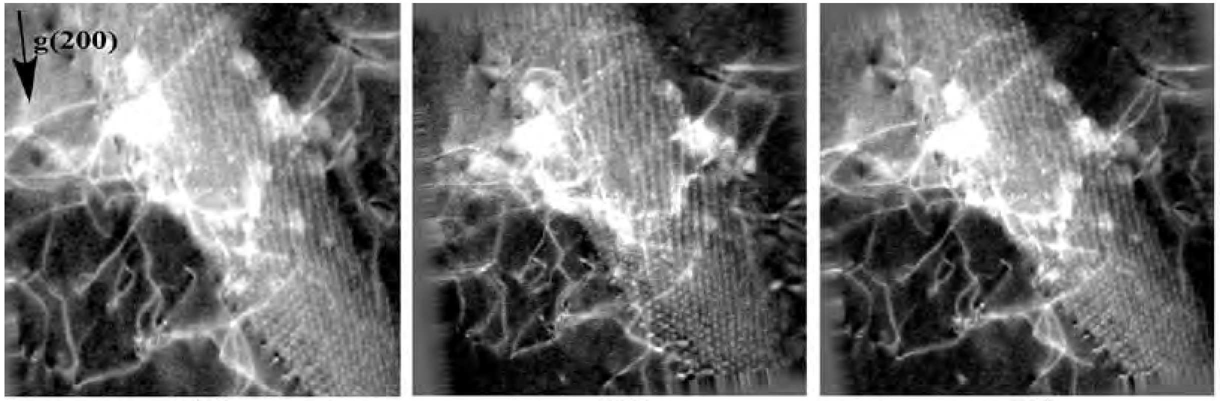

-44° -34° -22°

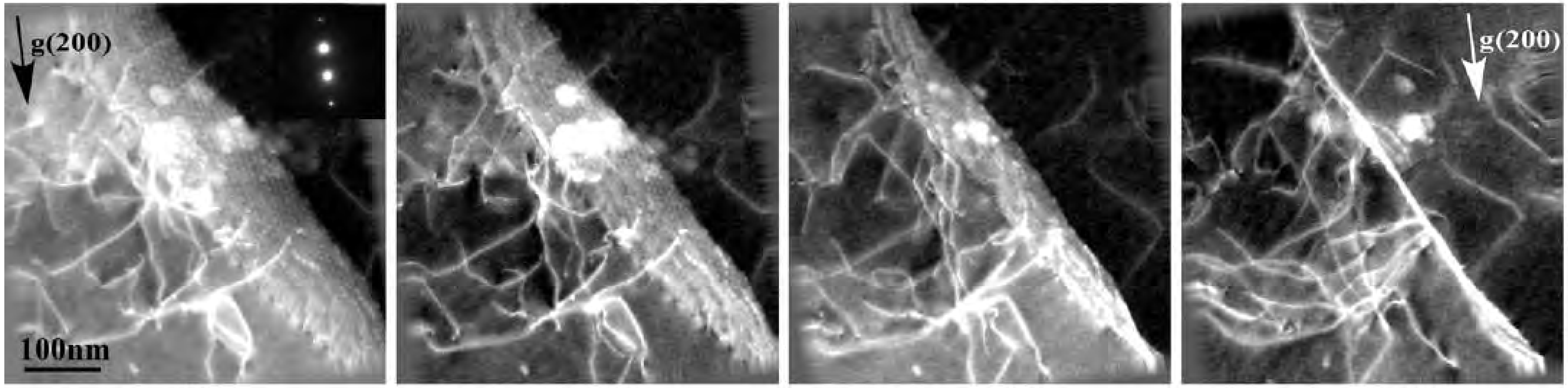

0° +8° +24° +48°

Fig. 3 shows a part of HAADF STEM tilt series of the planar boundary marked in Fig. 2 (in circle) taken at different alpha tilt angles using the two-beam condition for g (200).

Summary and future plan

1. 転位のTEMトモグラフィー観察法の発展

- ・高傾斜3軸ホルダーによる試料傾斜と回折条件設定の両立
- ・走査透過電子顕微鏡法STEMとトモグラフィーの相性：良
- ・実用材料への適用OK（磁性体は検討中）
- ・２軸トモグラフィーによる全転位可視化
- ・超高圧電子顕微鏡の利用

2. 今後の課題

- ・STEM転位像の3次元再構成像の理論的検討
- ・高速化、その場観察の可能性
- ・計算科学との融合
- ・直感に訴え、わかりやすい3次元像による顕微鏡学の進展と普及